Endothelial Wnt/β-catenin signaling inhibits glioma angiogenesis and normalizes tumor blood vessels by inducing PDGF-B expression

Marco Reis,[1] Cathrin J. Czupalla,[1] Nicole Ziegler,[1] Kavi Devraj,[1] Jenny Zinke,[1] Sascha Seidel,[1] Rosario Heck,[3] Sonja Thom,[1] Jadranka Macas,[1] Ernesto Bockamp,[3] Marcus Fruttiger,[4] Makoto M. Taketo,[5] Stefanie Dimmeler,[2] Karl H. Plate,[1] and Stefan Liebner[1]

[1]Institute of Neurology (Edinger Institute) and [2]Institute for Cardiovascular Regeneration, Johann Wolfgang Goethe University Frankfurt Medical School, 60590 Frankfurt am Main, Germany
[3]Division of Experimental and Translational Oncology, Department of Internal Medicine, Medical Center of the Johannes Gutenberg University Mainz, 55131 Mainz, Germany
[4]Institute of Ophthalmology–Cell Biology, University College London, London EC1V 9EL, England, UK
[5]Department of Pharmacology, Graduate School of Medicine, Kyoto University, Sakyo-ku, Kyoto 606-8501, Japan

Endothelial Wnt/β-catenin signaling is necessary for angiogenesis of the central nervous system and blood–brain barrier (BBB) differentiation, but its relevance for glioma vascularization is unknown. In this study, we show that doxycycline-dependent Wnt1 expression in subcutaneous and intracranial mouse glioma models induced endothelial Wnt/β-catenin signaling and led to diminished tumor growth, reduced vascular density, and normalized vessels with increased mural cell attachment. These findings were corroborated in GL261 glioma cells intracranially transplanted in mice expressing dominant-active β-catenin specifically in the endothelium. Enforced endothelial β-catenin signaling restored BBB characteristics, whereas inhibition by Dkk1 (Dickkopf-1) had opposing effects. By overactivating the Wnt pathway, we induced the Wnt/β-catenin–Dll4/Notch signaling cascade in tumor endothelia, blocking an angiogenic and favoring a quiescent vascular phenotype, indicated by induction of stalk cell genes. We show that β-catenin transcriptional activity directly regulated endothelial expression of platelet-derived growth factor B (PDGF-B), leading to mural cell recruitment thereby contributing to vascular quiescence and barrier function. We propose that reinforced Wnt/β-catenin signaling leads to inhibition of angiogenesis with normalized and less permeable vessels, which might prove to be a valuable therapeutic target for antiangiogenic and edema glioma therapy.

CORRESPONDENCE
Stefan Liebner:
stefan.liebner@kgu.de

Abbreviations used: α-SMA, α smooth muscle actin; BBB, blood–brain barrier; CM, conditioned medium; ColIV, collagen IV; DOX, doxycycline; EC, endothelial cell; GBM, glioblastoma; GOF, gain-of-function; HUVEC, human umbilical vein EC; IF, immunofluorescence; ISH, in situ hybridization; MBE, mouse brain endothelioma; mRNA, messenger RNA; PC, pericyte; PDGF-B, platelet-derived growth factor B; Podxl, podocalyxin; qRT-PCR, quantitative RT-PCR; SMC, smooth muscle cell; TJ, tight junction; VEGF, vascular endothelial growth factor.

Angiogenesis describes the growth of new blood vessels from preexisting ones and occurs during embryonic development and in the female reproductive cycle. In addition to physiological angiogenesis, vessel growth is closely associated with the progression of various tumors (Streit and Detmar, 2003). More specifically, the onset of tumor vascularization, known as angiogenic switch, defines progression to a highly malignant and eventually metastatic state (Bergers and Benjamin, 2003).

The vascular endothelial growth factor (VEGF) is crucial for physiological as well as pathological angiogenesis. VEGF, binding to the tyrosine kinase receptor VEGFR2 together with Nrp1 (neuropilin-1) and VEGFR3, requires the concerted interaction with other modulating pathways such as Notch, angiopoietin/Tie2, and ephrin/Eph to foster functional vessel growth (Adams and Alitalo, 2007). In tumors

C.J. Czupalla and N. Ziegler contributed equally to this paper.

S. Seidel's present address is Institute of Neuropathology, Justus Liebig University Medical School, 35392 Giessen, Germany.

The Rockefeller University Press $30.00
J. Exp. Med. 2012 Vol. 209 No. 9 1611-1627
www.jem.org/cgi/doi/10.1084/jem.20111580

The Journal of Experimental Medicine

however, VEGF overexpression downstream of HIF1α (hypoxia inducible factor 1 α) drives abnormal vessel growth and functions as a vascular permeability factor.

The WHO grade IV astrocytoma or glioblastoma (GBM) is one of the most vascularized and deadliest tumors (Machein and de Miguel, 2009). Because of its brain location, clinicians have to face specific complications such as loss of blood–brain barrier (BBB) characteristics in tumor vessels, leading to edema formation. Targeting glioma angiogenesis by VEGF inhibition had only minor impact on patient survival (Brastianos and Batchelor, 2009). Instead, it has been proposed that tumor vessel normalization rather than inhibition of angiogenesis is beneficial for tumor treatment, leading to reduced interstitial tumor pressure and metastasis and increased drug delivery (Carmeliet and Jain, 2011).

Beside VEGF, Notch, and other factors, the Wnt pathway has recently been shown to participate in developmental brain angiogenesis and in vascular differentiation to the BBB phenotype (Liebner et al., 2008; Stenman et al., 2008; Daneman et al., 2009). Wnts are glycosylated growth factors binding to receptors of the frizzled family (Smolich et al., 1993; Willert et al., 2003). Depending on the Wnt growth factor and the receptor context with Lrp5/6 coreceptors, signaling differs between the β-catenin/Lef/TCF (canonical) and the Ca^{2+}/protein kinase C or the planar cell polarity pathway (summarized as noncanonical; Chien et al., 2009). The Wnt/β-catenin pathway, which is understood best, has been implicated in developmental vasculo- and angiogenesis and in this context also in tip/stalk cell determination as well as in hereditary vascular diseases in humans (Franco et al., 2009; Phng and Gerhardt, 2009). In GBM, the noncanonical Wnt pathway driven by Wnt5a was shown to participate in tumor progression, most likely in a tumor cell–autonomous fashion (Kamino et al., 2011; Augustin et al., 2012). Although considerable information is available on tumor angiogenesis in general and on the role of VEGF herein, little is known about the canonical Wnt pathway in endothelial cells (ECs) under these conditions (Liebner and Plate, 2010).

Interestingly, Yano et al. (2000a,b) observed nuclear localization of β-catenin in tumor vessels of induced rat gliomas and of human GBM, suggesting a yet unknown involvement of endothelial Wnt/β-catenin signaling for brain tumor angiogenesis, although the function remained obscure. To address the function of the endothelial Wnt pathway for glioma angiogenesis, we stably transfected the mouse GL261 glioma cell line with Wnt1 or the soluble Wnt signaling inhibitor Dkk1 (Dickkopf-1). Surprisingly, Wnt1-expressing tumors were significantly smaller, vascular density was decreased, and investment with smooth muscle cells (SMCs) and pericytes (PCs) was augmented. This resulted in normalized and quiescent tumor vessels with increased barrier properties, indicated by junctional staining of tight junction (TJ) markers and decreased IgG leakage, respectively. A genetic gain-of-function (GOF) mouse model for endothelial β-catenin transcription corroborated these findings. Conversely, Dkk1-expressing tumors were bigger with higher vascular density and little attachment of SMCs/PCs to ECs.

Mechanistically, we provide evidence that activation of the Wnt/β-catenin pathway leads to the up-regulation of Dll4 (Delta-like 4) and increased Notch signaling in ECs during tumor neoangiogenesis. As a consequence of Wnt pathway activation, expression of tip cell genes was inhibited, whereas stalk cell genes were up-regulated, resulting in more quiescent ECs. Moreover, we show that transcriptional active β-catenin regulates the expression of platelet-derived growth factor B (PDGF-B) in the tumor endothelium, leading to increased SMC/PC coverage. In summary, our results provide the first evidence that enforced Wnt/β-catenin signaling reduces tumor angiogenesis on the one hand and augments SMC/PC recruitment via PDGF-B induction on the other, leading to a normalized glioma vessel phenotype with restored barrier properties.

RESULTS

The Wnt/β-catenin pathway is active in vessels of human glioma but does not correlate with tumor grade

As Wnt/β-catenin signaling has been shown to be active in vessels of human GBM by staining of nuclear β-catenin (Yano et al., 2000b), we wanted to evaluate whether gene expression of crucial Wnt pathway genes correlates with GBM. Analysis via the Texas Cancer Genome Analysis (TCGA) for selected Wnt pathway genes revealed up-regulated Wnt5a, a noncanonical factor, in human GBM (Fig. 1 A). Canonical Wnt factors, of which Wnt1, Wnt3a, and Wnt7a/b have been implicated in brain angiogenesis and BBB induction, were not regulated compared with normal brain. Interestingly, the soluble Wnt/β-catenin inhibitor Dkk1 showed in mean an elevation with big variability, whereas Dkk2, which has been proposed to have opposing function to Dkk1 in angiogenesis (Min et al., 2011), showed a contrary expression profile.

Staining for β-catenin of normal human brain sections revealed no nuclear staining of the protein in ECs, confirming our own previous results in adult mice (Fig. 1 B; Liebner et al., 2008). Compared with normal brain, several vessels in the tumor proper showed nuclear β-catenin localization but revealed no correlation with tumor grade (Fig. 1 C). However, the function of Wnt/β-catenin signaling in pathological angiogenesis has not been elucidated so far.

Wnt1 reduces subcutaneous glioma growth in NMRI-Foxn1^{nu} (NUDE) mice

To study the role of endothelial Wnt/β-catenin signaling in glioma angiogenesis, we established doxycycline (DOX)-inducible GL261 mouse glioma cell lines that upon DOX removal (−DOX) stably express either the empty vector (control^{-D}), mouse Wnt1 (Wnt1^{-D}), or human Dkk1 (Dkk1^{-D}). The induction of Wnt1 or Dkk1 expression was verified by Western blotting (Fig. 2 A), and the functional activity of the

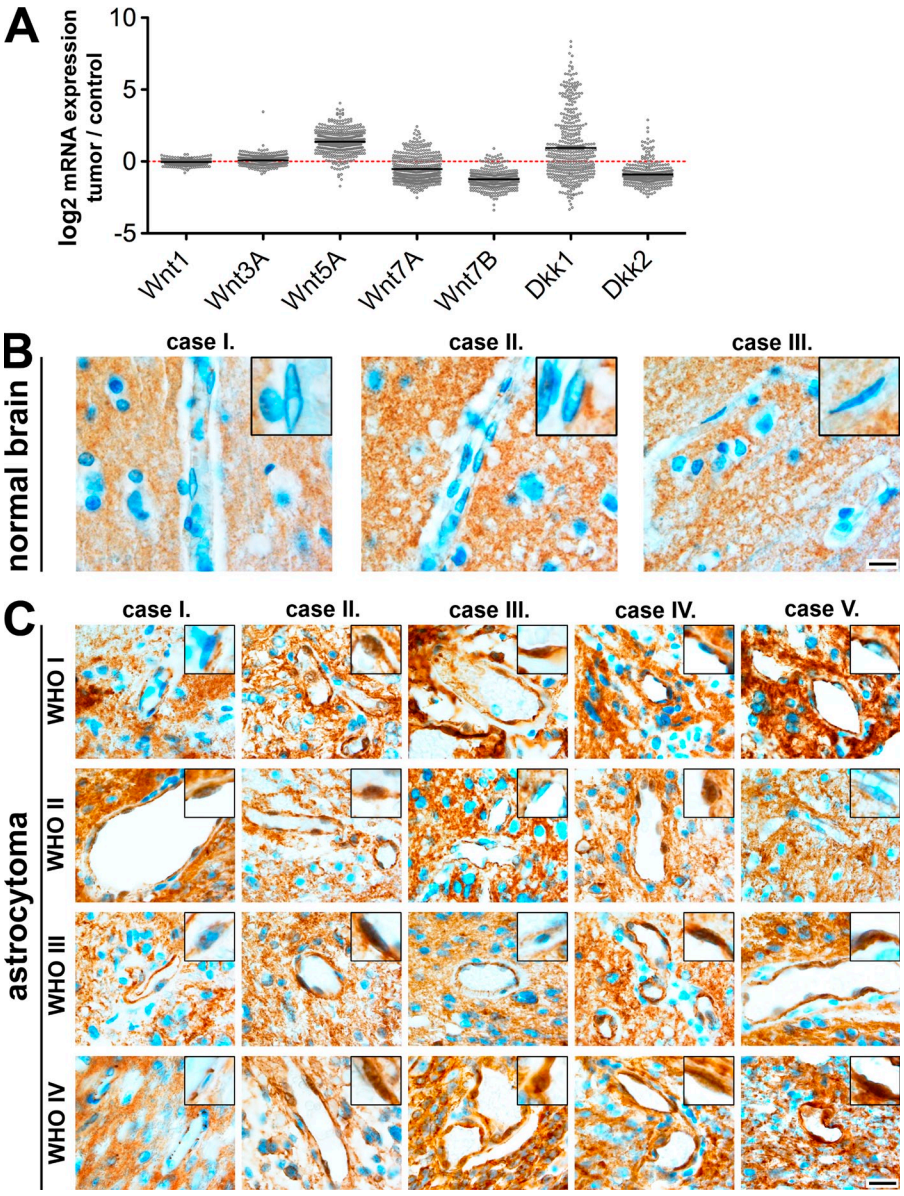

Figure 1. Nuclear β-catenin in vessels of human astrocytoma does not correlate with WHO grade. (A) TCGA database analyses for *Wnt1*, *Wnt3a*, *Wnt5a*, *Wnt7a*, *Wnt7b*, *Dkk1*, and *Dkk2* mRNA expression as log2-fold expression. Differences in mRNA expression in GBM compared with normal central nervous system tissue (dashed red line) are shown. (B and C) Paraffin sections of three normal human brains (B) and five different human astrocytoma WHO grades I–IV (C) stained for β-catenin and analyzed for its endothelial, nuclear localization. Insets show individual nuclei in higher magnification. Bars: (B) 14 µm; (C) 20 µm.

proteins was tested in co-cultures with HEK293 cells transfected with the sTOP/sFOP-FLASH reporter for β-catenin signaling (Fig. 2 B). Growth of Wnt1-GL261 cells showed the highest proliferation followed by Dkk1 and control cells. Notably, no growth differences could be observed by DOX administration (Fig. 2 C). A detailed characterization of these cell lines did not reveal significant differences in cell cycle, cell death, or in the expression of other Wnt ligands, including Wnt inhibitory proteins of the secreted frizzled-related protein family and Dkk family, as well as WIF1 (Wnt inhibitory factor-1; not depicted).

To evaluate tumor growth, we subcutaneously transplanted the GL261 lines in NUDE mice −DOX. During 20 d of growth, $Wnt1^{-D}$ tumors remained smaller, whereas $Dkk1^{-D}$ tumors were bigger compared with the controls (Fig. 2 D). Hematoxylin and eosin (H&E) staining on similar sized tumors revealed no obvious difference between the $control^{-D}$ and $Wnt1^{-D}$ condition (Fig. 2 E). Notably, necrotic areas with surrounding pseudopalisading cells were observed, suggesting that both tumors suffered from nutrition and oxygen deprivation. However, $Dkk1^{-D}$ tumors were rather compact with small necrotic areas (Fig. 2 E).

Hypoxia is increased in Wnt1- compared with Dkk1-expressing tumors. To evaluate tumor hypoxia, mice bearing similar sized tumors were injected with hypoxyprobe-1, revealing in $control^{-D}$ and $Wnt1^{-D}$ tumors pronounced hypoxia with no significant difference. $Dkk1^{-D}$ tumors showed significantly reduced hypoxic areas (Fig. 2 F), matching the few necrotic areas evaluated by tumor histology (Fig. 2 E). Because cell culture experiments showed no differences in proliferation (Fig. 2 C), cell cycle, and cell death between the three GL261 lines (not depicted), we hypothesized that Wnt1 and Dkk1 affect tumor vascularization, thus leading to differences in tumor growth. Wnt1 and Dkk1 functionally targeted the angiogenic endothelium in vivo, analyzed by nuclear localization of β-catenin in tumor vessels. Compared with $controls^{-D}$, the $Wnt1^{-D}$ tumor endothelium showed a significant increase in nuclear β-catenin, which is the hallmark of canonical Wnt signaling (Fig. 2 G). In contrast, nuclear β-catenin was decreased in $Dkk1^{-D}$ tumor vessels, suggesting that both Wnt1 and Dkk1 effectively stimulated the tumor endothelium.

Vessel density is decreased, wher2eas vessel stabilization is increased in Wnt1-expressing subcutaneous GL261 tumors

To exclude variations between the Wnt1- and Dkk1-expressing cell populations and to specifically show the effects of Wnt1 and

Dkk1 release on tumor growth, we repeated the initial subcutaneous tumor experiment with Wnt1- or Dkk1-GL261 lines in the presence or absence of DOX (+D, −D). In the presence of Wnt1 expression (Wnt1^{-D}), GL261 tumors grew significantly smaller and mouse survival was increased (Fig. 3 A). On Dkk1-GL261 tumors, DOX withdrawal (Dkk1^{-D}) had the opposite effect (Fig. 3 B), confirming the finding of the initial comparison between control^{-D}, Wnt1^{-D}, and Dkk1^{-D}

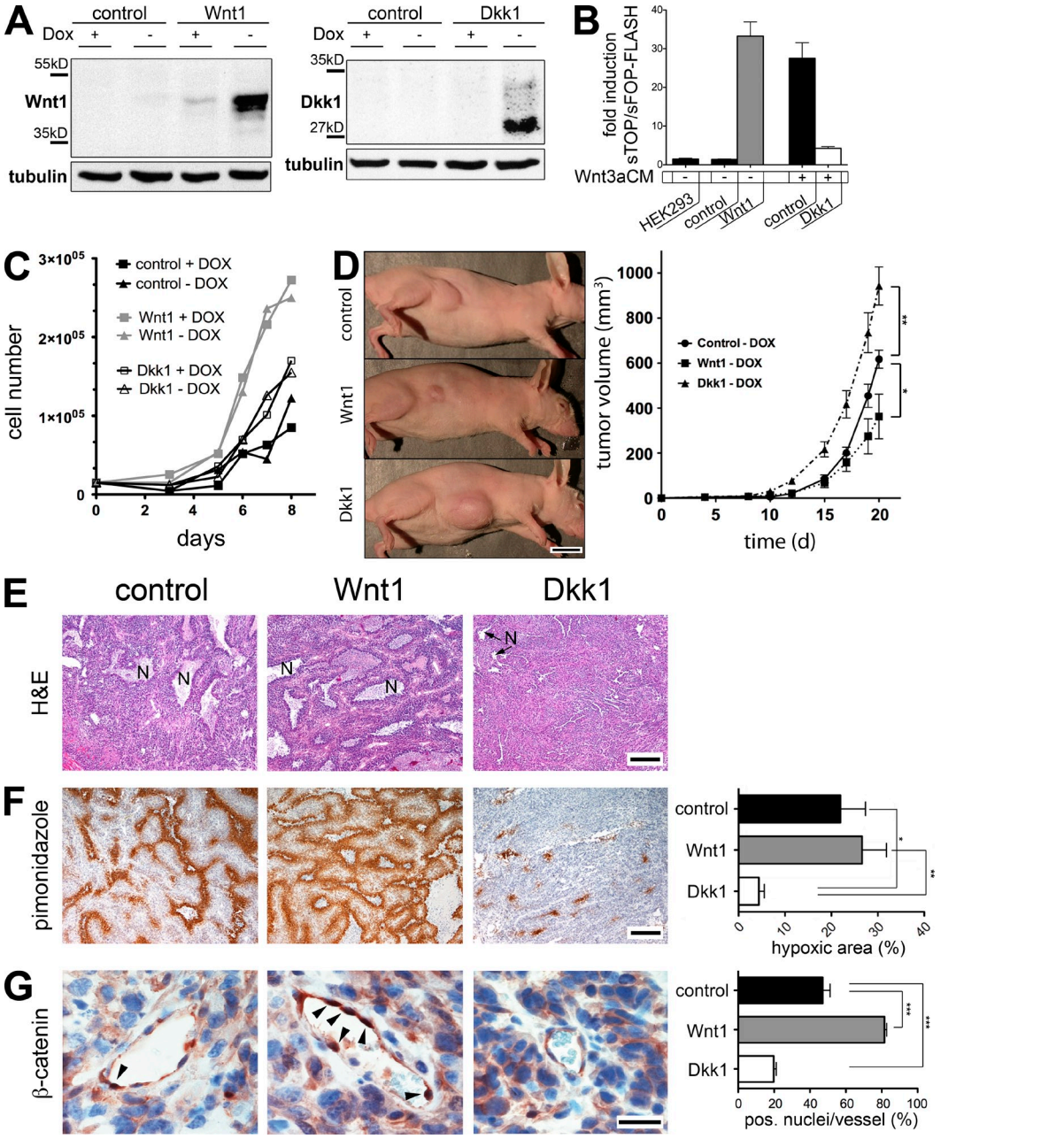

Figure 2. Wnt1 expression decreased subcutaneous GL261 tumor growth and increased animal survival. (A) Western blots showing Wnt1 and Dkk1 expression +/−DOX in GL261 cells. (B) sTOP-FLASH assay on human embryonic kidney (HEK293)/GL261 co-cultures without DOX. Monoculture of transfected HEK293 cells served as baseline. Wnt1 and Dkk1 cells were cultured without (−) or with (+) Wnt3aCM (one experiment in triplicate). (C) In vitro proliferation of the control-, Wnt1-, and Dkk1-GL261 line cultured +/−DOX. (D, left) Representative pictures of NUDE mice with subcutaneous tumors −DOX. (right) Tumor volumes (n = 7/group) of the transplanted glioma cell lines −DOX (*, $P < 0.05$; **, $P < 0.01$). (E) H&E-stained paraffin sections revealed reduced necrotic areas for Dkk1-expressing tumors (N). (F, left) Pimonidazole (brown) immunohistochemistry staining revealed tumor hypoxia, hematoxylin counterstaining (blue). (right) Hypoxia in Dkk1^{-D} compared with the control^{-D} (*, $P < 0.05$) and Wnt1^{-D} tumors (**, $P < 0.01$; n = 4 tumors/group, slices from the center of similar sized tumors). (G, left) Representative vessels, stained for nuclear β-catenin (brown) and hematoxylin (blue) of control^{-D}, Wnt1^{-D}, and Dkk1^{-D} tumors. Arrowheads point to β-catenin^{+} nuclei. (right) Quantification of β-catenin^{+} nuclei (n = 4 tumors/group, 20 vessels/tumor; ***, $P < 0.001$). Bars: (D) 1 cm; (E and F) 400 µm; (G) 35 µm. Error bars indicate SEM.

tumors (Fig. 2 D) and arguing for a specific, expression-dependent effect of Wnt1 and Dkk1.

We investigated tumor vessel density and morphology by staining for the endothelial marker CD31/PECAM-1 and α smooth muscle actin (α-SMA; Fig. 3, C and D). Interestingly, $Wnt1^{-D}$ tumors showed decreased vessel density compared with $Wnt1^{+D}$ (Fig. 3 C), whereas in $Dkk1^{-D}$ tumors vessel density was increased (Fig. 3 D). The vessel reduction in $Wnt1^{-D}$ tumors was accompanied by increased attachment of $\alpha\text{-SMA}^+$ cells (Fig. 3 C). Notably, in Dkk1 tumors in general, $\alpha\text{-SMA}^+$ cells were frequently detached from the tumor endothelium and were regularly detected in the tumor stroma, showing no difference upon DOX treatment (Fig. 3 D). From the images in Fig. 3 (C and D) it can be deduced that the size of tumor vessels was increased in the $Wnt1^{-D}$ group as compared with the $Wnt1^{+D}$ and $Dkk1^{+/-D}$ groups (see also Fig. 8 B). To determine functionality of tumor blood vessels, mice were perfused with isolectin, revealing that the majority of vessels from control^{-D}, $Wnt1^{-D}$, and $Dkk1^{-D}$ tumor groups exhibited blood flow (Fig. 3 E). The effects of Wnt1 on tumor vascularization and growth in the subcutaneous transplantation paradigm could be confirmed independently by a C6 rat glioma cell line stably expressing Wnt1 (not depicted).

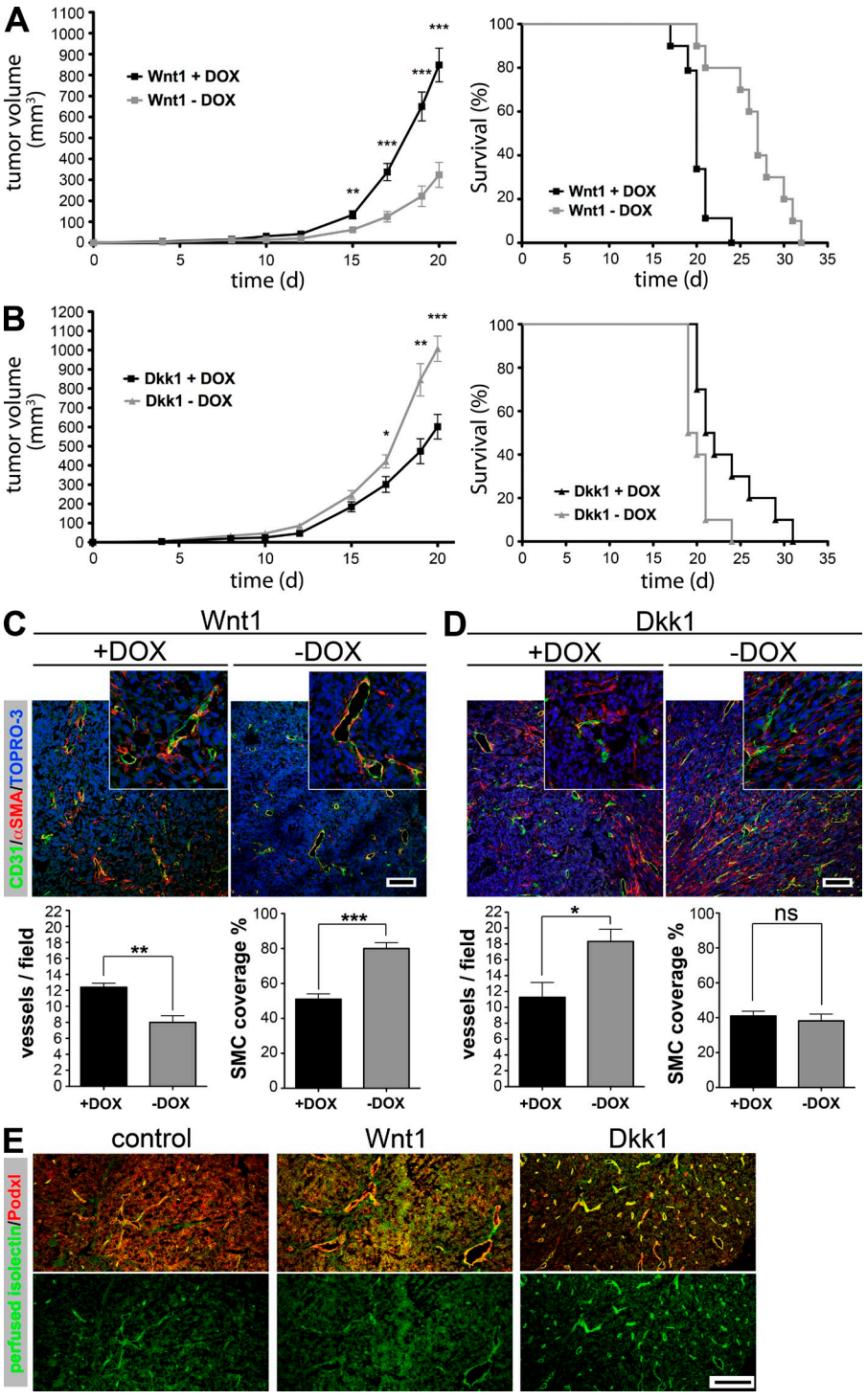

Antiangiogenic and vessel-normalizing effect of β-catenin signaling is EC autonomous

To understand whether Wnt1 and Dkk1 have angiogenic effects in a tumor cell–free angiogenesis paradigm, we performed in vivo Matrigel

Figure 3. Tumor-derived Wnt1 reduced and normalized subcutaneous tumor vascularization, whereas Dkk1 caused the opposite effect. (A) Tumor growth in $Wnt1^{-D}$ compared with $Wnt1^{+D}$ condition (left; $n = 12$/group; **, $P < 0.01$; ***, $P < 0.001$) and mouse survival (right; $n = 12$/group). (B) Tumor volume for $Dkk1^{-D}$ compared with $Dkk1^{+D}$ condition (left; $n = 12$/group; *, $P < 0.05$; **, $P < 0.01$; ***, $P < 0.001$) and mouse survival of $Dkk1^{+/-D}$ tumors (right; $n = 12$/group). (C, top) IF staining on subcutaneous Wnt1 tumors for CD31/PECAM-1, α-SMA, and TOPRO-3. (bottom left) Vessel density of subcutaneous Wnt1 tumors +/−DOX ($n = 5$ tumors/group, 10 pictures/tumor; **, $P < 0.01$). (bottom right) Association of $\alpha\text{-SMA}^+$ cells to ECs in $Wnt1^{+/-D}$ tumors ($n = 5$ tumors/group, 10 vessels/tumor; ***, $P < 0.001$). (D) Same staining and experimental settings as in C for subcutaneous $Dkk1^{+/-D}$ tumors (*, $P < 0.05$). (C and D) Insets show vessels in higher magnification. (E) Perfusion with isolectin revealed that vessels from control^{-D}, $Wnt1^{-D}$, and $Dkk1^{-D}$ tumors exhibited blood flow. Bars: (C and D) 400 µm; (E) 200 µm. Error bars indicate SEM.

plug assays. For this purpose, Matrigel plugs were supplemented with recombinant Wnt1 or Dkk1 protein and injected in C57BL/6 mice, which were sacrificed after 7 d. Vessel density was analyzed by measuring the CD31/PECAM1-positive ($CD31^+$) area in relation to the plug area. Compared with controls, the $CD31^+$ area was decreased in Wnt1 and increased in Dkk1 Matrigel plugs, confirming the finding in GL261 tumors that Wnt1 decreased and Dkk1 fostered angiogenesis (Fig. 4, A and B).

Wnt1 expression leads to quiescent vessels and reduces tumor volume and IgG leakage in intracranial transplantations

To evaluate orthotopic growth, vascularization, and BBB characteristics of glioma vessels, we transplanted the engineered GL261 cell lines into the striatum of NUDE mice (Fig. 5 A). Consistent with the subcutaneous tumor experiments, $Wnt1^{-D}$ tumors grew the slowest and the volume was notably decreased compared with $controls^{-D}$ and even more pronounced compared with the $Dkk1^{-D}$ glioma (Fig. 5 B).

Vascular density was also significantly reduced in intracranial $Wnt1^{-D}$ tumors (Fig. 5, A and B). We further characterized GL261 glioma vessels for PC coverage by staining for desmin. Consistent with the subcutaneous paradigm, the vessels of $Wnt1^{-D}$ showed significantly augmented attachment of $desmin^+$ cells, supporting a normalized vascular morphology (Fig. 5 C).

Wnt/β-catenin signaling as well as PCs have been shown to be important for the establishment and maintenance of the BBB (Armulik et al., 2010; Daneman et al., 2010). Therefore, we investigated whether endothelial barrier properties are affected by modulating the Wnt pathway in experimental glioma by staining thick sections of tumor-bearing brains for endogenous mouse IgG, which is frequently used as a marker for BBB disruption. Confocal imaging and large image reconstruction revealed strong IgG leakage into the tumor and the surrounding brain parenchyma in $control^{-D}$ and $Dkk1^{-D}$ glioma, which was substantially reduced in $Wnt1^{-D}$ tumor-bearing brains (Fig. 5 D). Notably, in $control^{-D}$ and $Dkk1^{-D}$ brains, IgG was detectable around the lateral ventricles and on the contralateral hemisphere. Instead, for $Wnt1^{-D}$ tumors this was not observed. Higher magnifications confirmed weaker IgG staining also in the immediate circumference of podocalyxin (Podxl)-positive ($Podxl^+$) vessels in $Wnt1^{-D}$ tumors, suggesting that these vessels retained or regained barrier properties (Fig. 5 D).

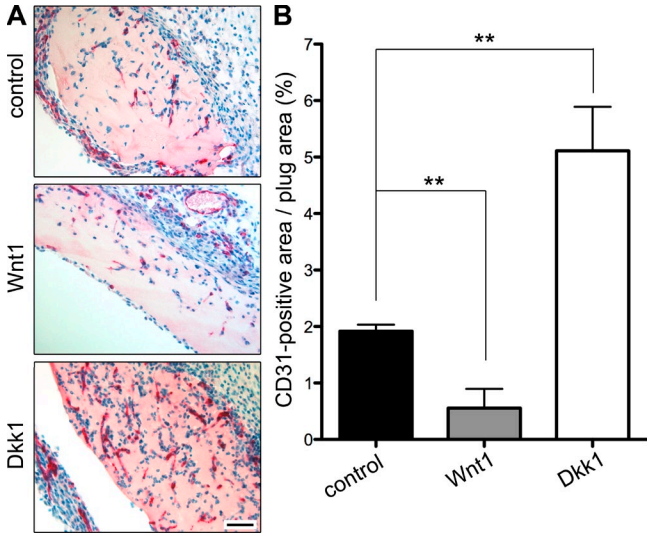

Figure 4. Tumor cell–free Matrigel plug assay confirmed the anti-angiogenic effect observed in Wnt1-GL261 tumors. (A) Immunohistochemistry staining for CD31/PECAM-1 (red) and hematoxylin counterstaining (blue) of Matrigel plug sections, supplemented with diluent (control), 400 µg/ml human Wnt1, or 200 µg/ml mouse Dkk1 recombinant proteins. Bar, 200 µm. (B) Quantification of $CD31^+$ area in percentage in Matrigel plugs (n = 6 plugs/group, 8 representative pictures/plug; **, $P < 0.001$). Error bars indicate SEM.

Endothelial Wnt/β-catenin signaling partially rescues the loss of BBB junction markers in GL261 glioma vessels

The TJ protein Cldn3 (claudin-3) has previously been shown to become down-regulated in several brain pathologies such as tumors and inflammation, and it has been identified as a Wnt/β-catenin target in ECs (Wolburg et al., 2003; Liebner et al., 2008). Stainings for Cldn3 together with the endothelial marker CD31/PECAM-1 showed that CD31 was localized at cell–cell junctions of tumor vessels in the three tumor types (Fig. 6 A), whereas Cldn3 showed a punctuate staining only occasionally overlapping with the $CD31^+$ areas in $control^{-D}$ and $Dkk1^{-D}$ tumors. Instead, in $Wnt1^{-D}$ tumors more continuous, junctional staining of Cldn3 that colocalized with CD31 was observed, arguing for more elaborate TJs as observed in physiological brain vessels. In tumor vessels of $Wnt1^{-D}$ glioma, other junctional markers such as Cldn5 and ZO-1 (zonula occludens 1) also showed more restricted junctional staining (Fig. 6 B).

Endothelial-specific activation of β-catenin signaling results in vessel quiescence of intracranial GL261 tumors

We further asked whether dominant endothelial-specific activation of β-catenin signaling can mimic the effects observed in Wnt1-expressing tumors. Therefore, we generated mice expressing a dominant-active form of β-catenin specifically in the endothelium (GOF) and intracranially transplanted the parental, not engineered GL261 glioma cells. In brief, we made use of the Pdgfb-iCreERT2 mice crossed to the $\beta\text{-catenin}^{Exon3flox/flox}$ line as previously described (Liebner et al., 2008). The mice were sacrificed when the first animals showed symptoms (see Materials and methods). Recombination was induced by subcutaneously transplanted tamoxifen pellets (free base) on the same day of tumor transplantation. Recombination of intracranial tumor vessels was evaluated by crossing Pdgfb-iCreERT2 and $ROSA26^{STOPfloxLacZ}$ mice. Staining for Podxl and β-galactosidase revealed endothelial recombination of ∼30% (Fig. 7 A).

In the GOF (Pdgfb-iCreERT2 × $\beta\text{-catenin}^{Exon3flox/flox}$ + tamoxifen) tumors, we observed reduced vessel density compared

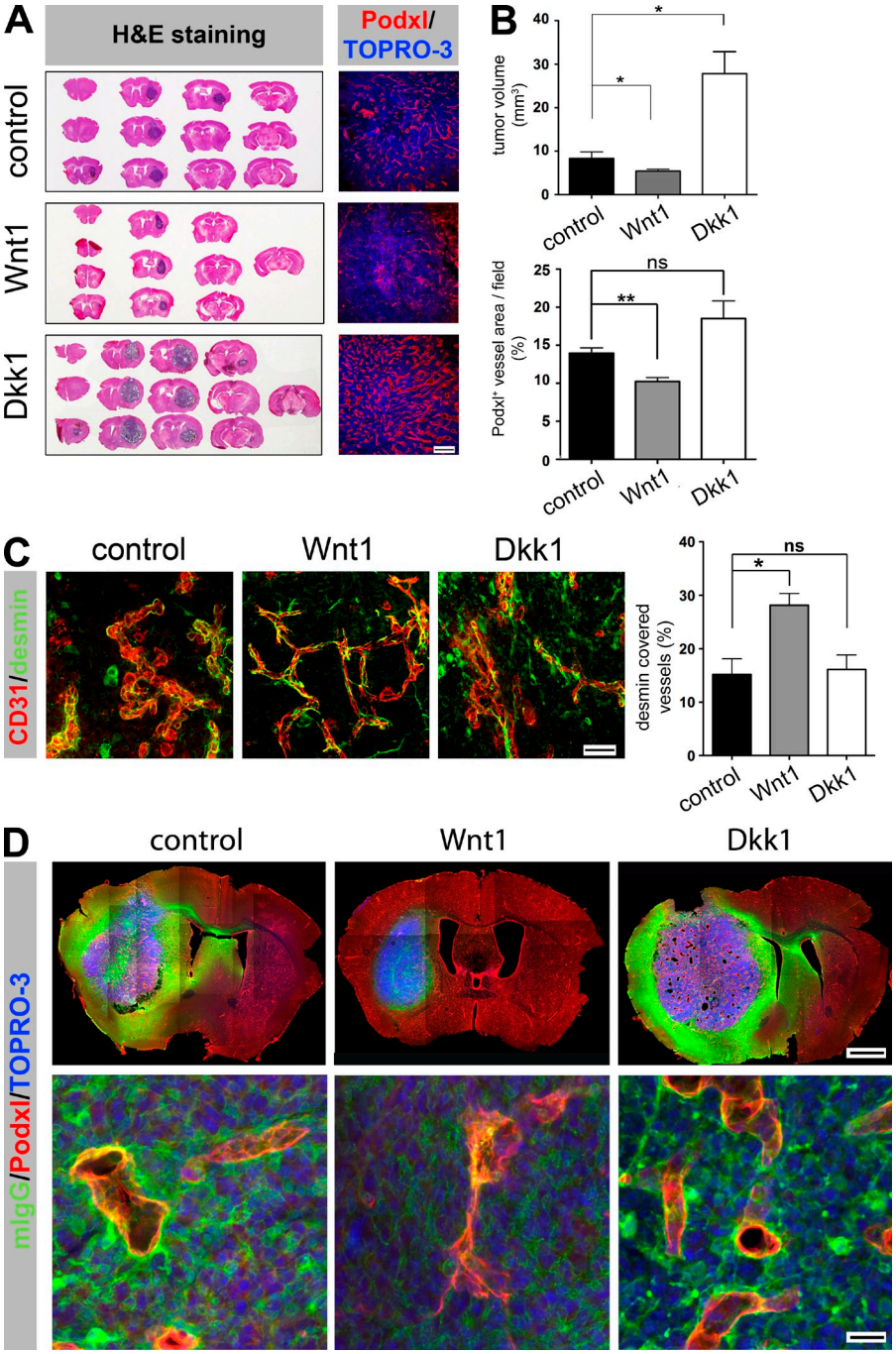

Figure 5. Tumor-derived Wnt1 normalized vascularization and retained vascular barrier properties in GL261 glioma. (A, left) Representative H&E staining of serial thick sections of tumor-bearing mouse brains. (right) Corresponding IF staining for Podxl and TOPRO-3. (B, top) Quantification of glioma volume based on H&E staining (control^{-D} $n = 3$, Wnt1^{-D} $n = 6$, and Dkk1^{-D} $n = 4$; *, $P < 0.05$). (bottom) Podxl^{+} vessel areas within tumors (control $n = 4$, Wnt1 $n = 6$, Dkk1 $n = 5$; **, $P < 0.01$). (C) IF staining for CD31/PECAM-1 and desmin ($n = 3$ tumors/group, 8 pictures/tumor; *, $P < 0.05$). (D) Large image reconstructions of IF staining for mouse endogenous IgG (mIgG), Podxl, and TOPRO-3 on brain sections bearing control^{-D}, Wnt1^{-D}, and Dkk1^{-D} glioma. Bars: (A) 200 µm; (C) 50 µm; (D, top) 1 mm; (D, bottom) 27 µm. Error bars indicate SEM.

with the controls (Pdgfb-iCreERT2 + tamoxifen; Fig. 7 B). Interestingly, the basal lamina of control tumor vessels regularly showed a rough distribution around the endothelium, whereas in the GOF condition it had a smooth appearance as revealed by collagen IV (ColIV) staining, speaking for a more quiescent vessel phenotype (Fig. 7 C and Videos 1 and 2). Indeed, ColIV was more closely distributed around the vascular wall in the GOF tumor vessels, as indicated by a lower ratio of ColIV to Podxl (Fig. 7 C). The normalized vessel phenotype in GOF tumors was further underlined by increased desmin^{+} cells attached to the endothelium (Fig. 7 D and Videos 3 and 4). We next asked for the mechanism by which endothelial Wnt/β-catenin signaling hampers tumor angiogenesis, leading to the quiescent and normalized vessel phenotype described above.

Wnt/β-catenin signaling results in Dll4 expression and a stalk cell gene signature

The Notch pathway via Notch1/4 and Dll4 has been shown to be a key regulator in vessel sprouting by inhibiting the tip cell and promoting the stalk cell phenotype (Phng and Gerhardt, 2009). Recently, Corada et al. (2010) could show that β-catenin signaling regulates Dll4 during early embryonic angiogenesis but becomes silenced during late embryonic and postnatal development.

To understand whether endothelial Wnt/β-catenin signaling regulates Dll4 also in the tumor endothelium, we performed Dll4 in situ hybridization (ISH). Hematoxylin counterstaining revealed tumor vessel–specific Dll4 expression in all three tumor conditions (Fig. 8 A). Analysis of vessel diameter revealed significantly decreased small and increased big vessels for Wnt1^{-D} tumors, as opposed to the vascular phenotype in Dkk1^{-D} tumors (Fig. 8 B). Interestingly, in all tumor conditions small vessels were positive for Dll4, which is in line with an endothelial tip cell characteristic described in a previous publication (Hellström et al., 2007). In this regard, it was apparent that in Wnt1^{-D} tumors

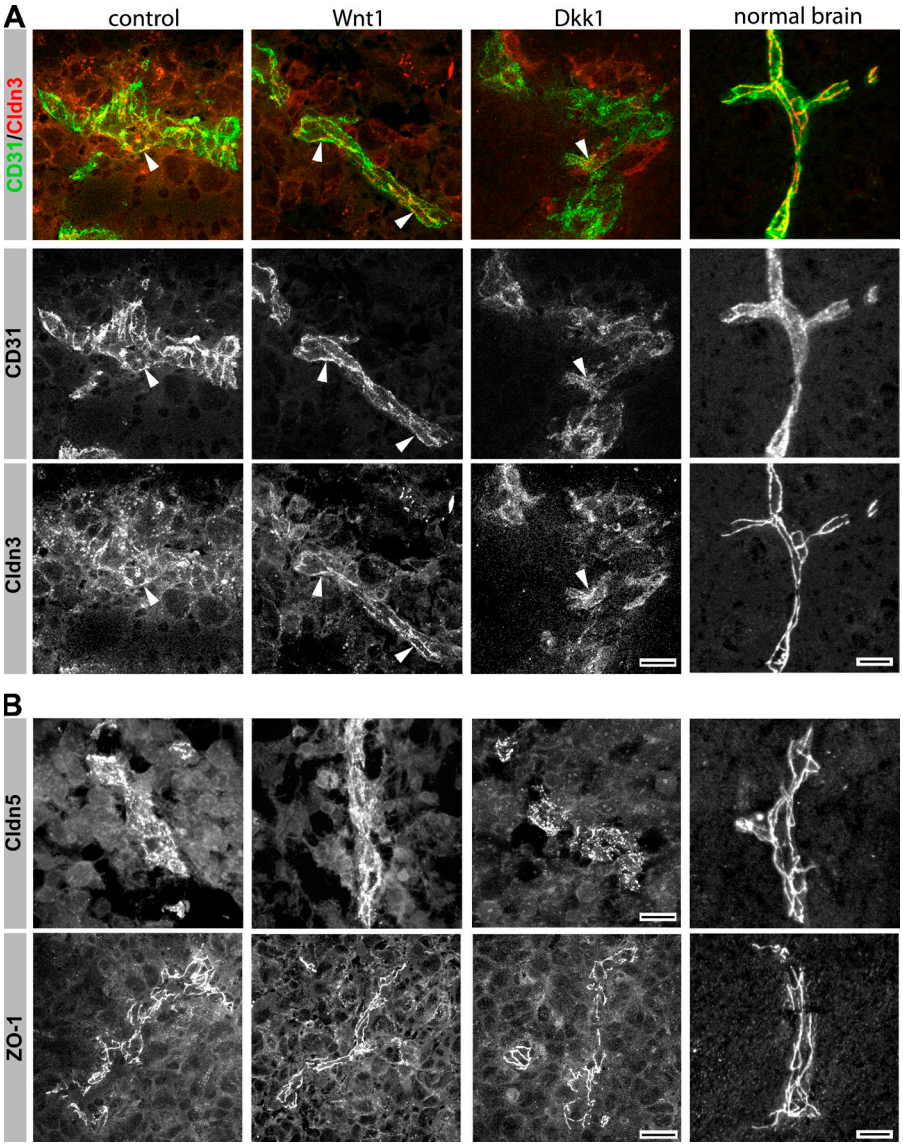

Figure 6. Cldn3, Cldn5, and ZO-1 showed junctional localization in vessels of Wnt1-expressing GL261 gliomas. (A) IF staining for CD31/PECAM and Cldn3 on GL261 glioma and normal brain sections. Arrowheads indicate junctional localization. (B) IF staining for Cldn5 and ZO-1 on cryosections of GL261 brain tumors and normal brain. Bars: (A and B, tunors) 33 µm; (A and B, normal brain) 10 µm.

bigger vessels >300 µm^2 were also strongly positive for Dll4, which was not the case in controls^{-D} and specifically not in Dkk1^{-D} tumors (Fig. 8 B).

To test whether GL261-derived Wnt1 directly induces Dll4 expression in ECs, we established a co-culture system of GL261 cells with human umbilical vein ECs (HUVECs; Fig. 8 C). Using human-specific primers, quantitative RT-PCR (qRT-PCR) analysis revealed significant up-regulation of *AXIN2*, an endogenous Wnt target gene, and *DLL4* in Wnt1^{-D}/HUVEC compared with control^{-D}/HUVEC co-cultures, which was not the case in Dkk1^{-D}/HUVECs (Fig. 8 C). In addition to *DLL4*, we also observed an up-regulation of *JAG1* (*jagged-1*) and of the Notch target *NRARP* (*Notch-related ankyrin repeat protein*), whereas other targets such as *HES1* (*hairy and enhancer of split homologue 1*) and *HEY* (*hairy/enhancer of split related with YRPW motif*) were not significantly regulated. In Dkk1^{-D} co-cultures except for *JAG1*, none of the tested genes were up-regulated, but *NRARP* was significantly down-regulated.

One of the key pathways to modulate vascular activation is the angiopoietin-Tie2 system. In particular, *ANGPT2* (*angiopoietin-2*), which is highly expressed in angiogenic ECs, leads to SMC/PC drop out and vascular instability (Thomas and Augustin, 2009). In HUVEC co-cultures, neither Wnt1 nor Dkk1 produced by GL261 cells had a significant effect on endothelial *ANGPT2* expression (Fig. 8 C). In turn, GL261-derived, murine *Angpt1* was also not regulated in Wnt1^{-D} and Dkk1^{-D} co-culture conditions (not depicted). Analysis of total RNA from subcutaneous GL261 tumors revealed a diminished expression of *Angpt2* specifically in Wnt1^{-D} glioma when normalized to the endothelial-specific gene VE-cadherin, supporting the more quiescent phenotype in these tumors (not depicted).

To understand the expression of Notch pathway genes downstream of Wnt/β-catenin in more detail, we stimulated mouse brain endotheliomas (MBEs) with Wnt3a conditioned medium (CM [Wnt3aCM]; Liebner et al., 2008). Wnt3aCM robustly induced *Axin2* and *Dll4* expression as well as the Notch targets *Hes1* and *Hey1* after 18 h of stimulation (Fig. 8 D). *Jag1*, *Notch1*, and *Nrarp* were not changed at this time point, whereas *Flt-1* (*VEGFR1*), a putative VEGF-A decoy receptor, showed significant up-regulation. Other Notch targets showed no significant regulation, which was also true for arterial genes such as ephrinB2 (not depicted). However, after 48 h of stimulation (Fig. 8 D), Jag1 and Notch1 were significantly up-regulated, whereas *Nrp-1* and *Flt4* (*VEGFR3*) were down-regulated.

Transcriptionally active β-catenin regulates expression of PDGF-B in ECs in vitro

Finally, we intended to clarify the mechanism leading to increased tumor vessel attachment of vascular SMCs/PCs upon

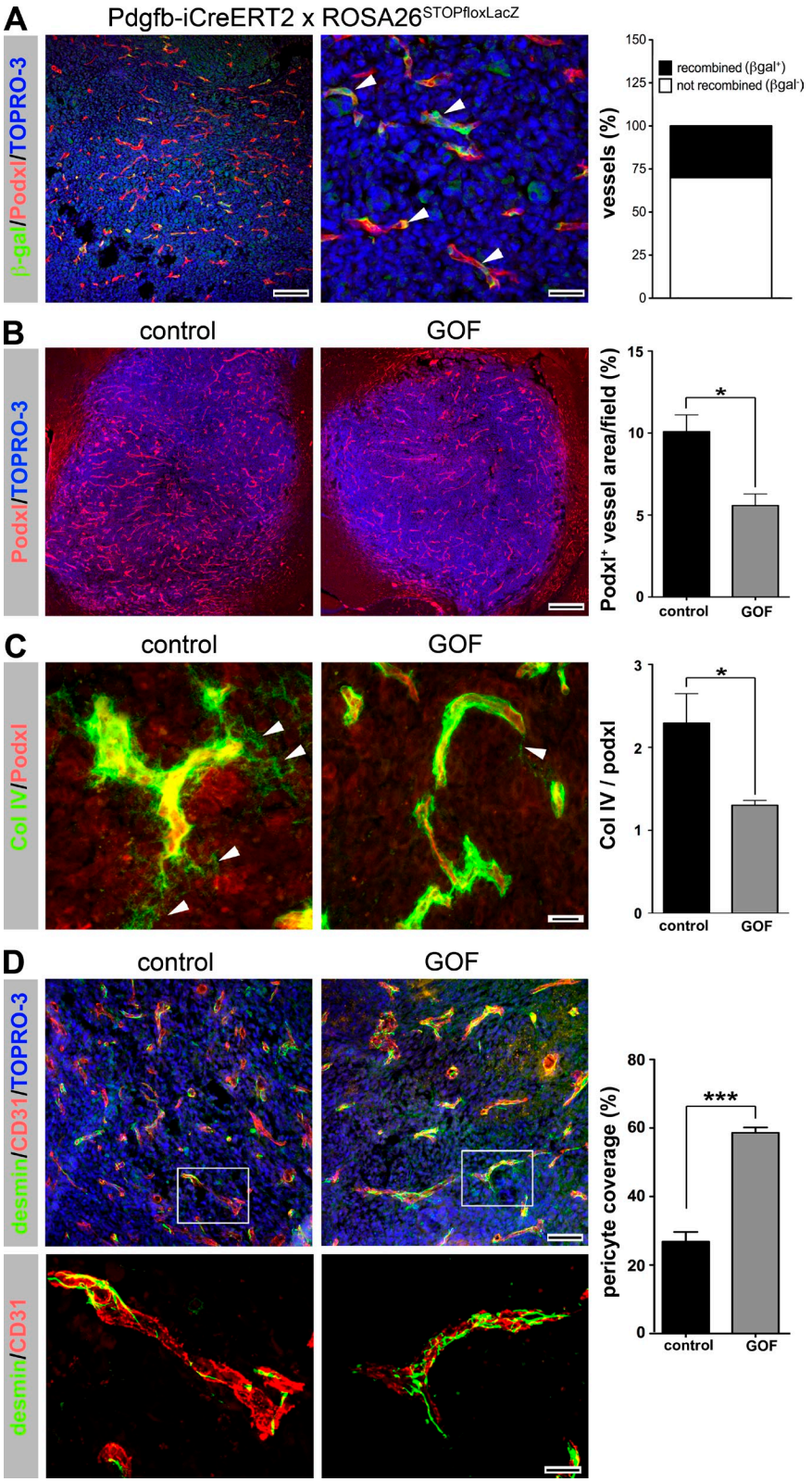

Figure 7. Vascular effects observed in Wnt1-expressing gliomas are EC autonomous. (A, left) IF staining for β-galactosidase (β-gal), Podxl, and TOPRO-3 on GL261 glioma sections from Pdgfb-iCreERT2 × ROSA26^{STOPfloxLacZ} mice treated with tamoxifen. (right) Quantification of β-gal$^+$ vessels. (B, left) IF staining for Podxl and TOPRO-3 on GL261 glioma sections from Pdgfb-iCreERT2 (control) and Pdgfb-iCreERT2 × βCat^{Ex3flox} (GOF) mice. (right) Quantification of Podxl$^+$ areas within tumors ($n = 4$ tumors/group, 10 pictures/tumor; *, $P < 0.05$). (C, left) ColIV and Podxl staining of tumor sections from control and GOF mice. Arrowheads point to nonendothelial-associated ColIV$^+$ structures. (right) ColIV/Podxl ratio ($n = 4$ tumors/group, 8 pictures/tumor; *, $P < 0.05$). (D, top left) IF staining for CD31/PECAM-1 and desmin on tumor sections from control and GOF mice ($n = 4$ tumors/group, 10 pictures/tumor). (right) Quantification of PC coverage (***, $P < 0.001$). (bottom left) Representative vessel in higher magnification (white boxes). Bars: (A [left] and D [top]) 160 µm; (A, right) 40 µm; (B) 400 µm; (C and D [bottom]) 20 µm. Error bars indicate SEM.

endothelial Wnt/β-catenin activation. As *ANGPT2* was not significantly regulated upon canonical Wnt pathway activation in the HUVEC co-culture setting, we investigated the regulation of *PDGFB* as the best known SMC/PC attractant produced by the endothelium and observed a significant up-regulation of *PDGFB* messenger RNA (mRNA) in the presence of Wnt1-expressing GL261 cells (Fig. 9 A). Comparable results were obtained by Wnt3a stimulation of MBEs after 18 and 48 h (Fig. 9 B).

To understand whether the *Pdgfb* gene is directly regulated by transcriptionally active β-catenin, we generated EC lines derived from β-catenin–deficient endothelioma cells (Cattelino et al., 2003), expressing a chimeric construct of Lef1 and the transactivation domain of β-catenin (LefΔN-βCTA), conferring dominant-active transcription without affecting the membrane function of β-catenin or the corresponding vector control (Vleminckx et al., 1999). LefΔN-βCTA strongly induced *Axin2* as an endogenous reporter gene and *Pdgfb* as indicated by qRT-PCR analysis. Western blot analysis revealed an up-regulation of PDGF-B and the homodimer PDGF-BB by ∼60%, suggesting that protein translation is also taking place (Fig. 9 C).

To further characterize whether Pdgfb expression downstream of β-catenin transcription is dependent on subsequent

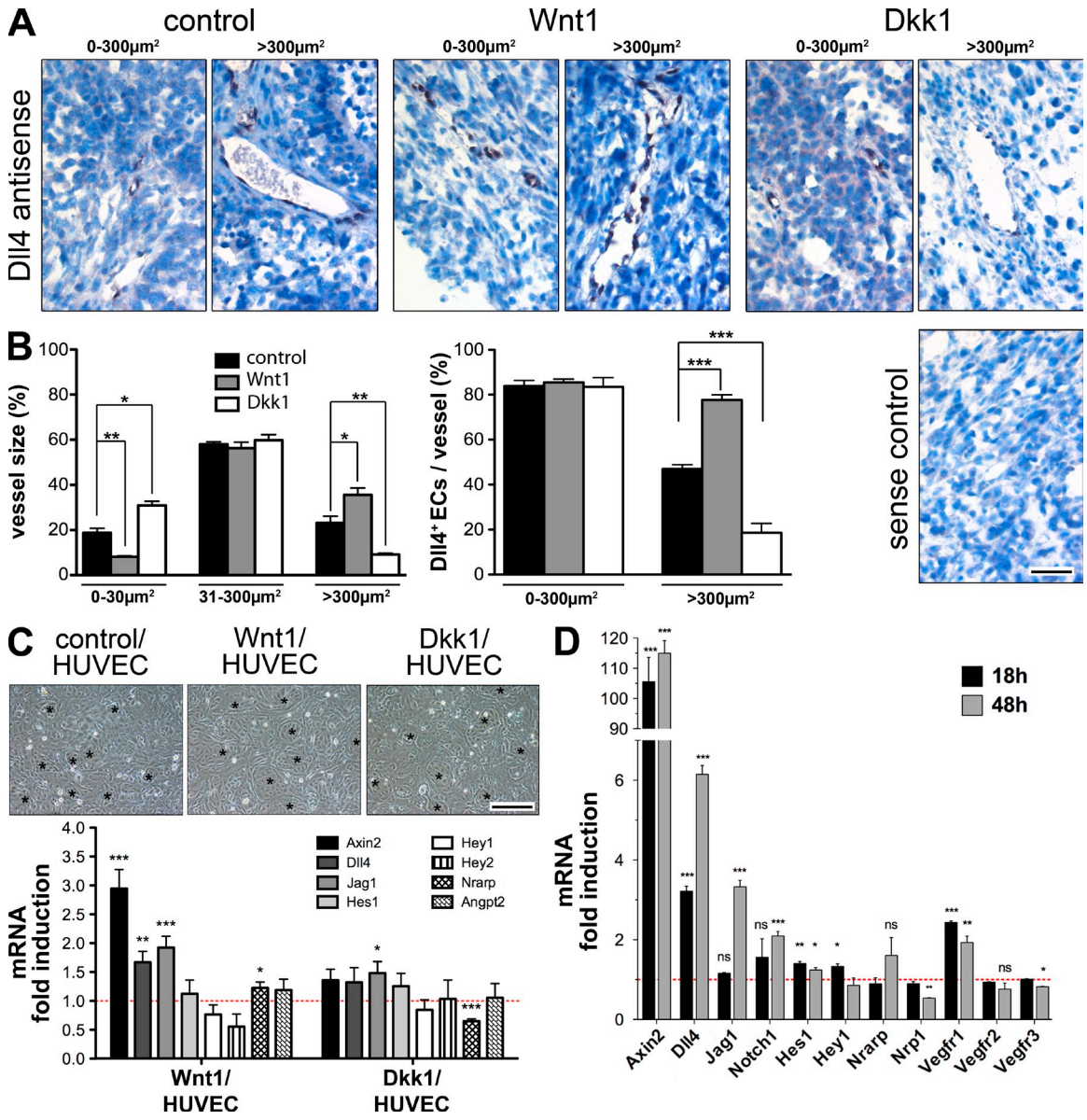

Figure 8. Glioma-derived Wnt1 up-regulated endothelial *Dll4*, leading to a stalk cell–like gene signature. (A) ISH against *Dll4* (black) and hematoxylin (blue) of subcutaneous control^{-D}, Wnt1^{-D}, and Dkk1^{-D} GL261 tumors, showing representative small (0–300 µm²; left) and large (>300 µm²; right) vessels. (B, left) Quantification of vessel diameter (n = 3 tumors/group, 15 pictures/tumor) grouped in categories of 0–30 µm², 31–300 µm², and >300 µm² (*, P < 0.05; **, P < 0.01). (right) Quantification of Dll4⁺ ECs (n = 6 tumors/group, 5 small and 5 large vessels/tumor; ***, P < 0.001). (C, top) HUVECs co-cultivated with control^{-D}, Wnt1^{-D}, and Dkk1^{-D} GL261 cells (asterisks indicate HUVECs). (bottom) qRT-PCR (n = 6) for human genes regulated by Wnt1^{-D} and Dkk1^{-D} compared with control^{-D} co-cultures (red line). (D) qRT-PCR for mouse genes regulated in MBEs stimulated by Wnt3aCM for 18 and 48 h compared with controlCM (red line; n = 3; *, P < 0.05; **, P < 0.01; ***, P < 0.001). Bars: (A) 50 µm; (C) 80 µm. Error bars indicate SEM.

Notch pathway activation, we analyzed β-catenin–deficient cells grown on Dll4-coated dishes or on gelatin as a control with and without LefΔN-βCTA expression. In addition, the Notch pathway was blocked by a Dll4-Fc fragment (Lobov et al., 2007). We could confirm that Dll4 coating induced Notch pathway activation as indicated by Hes1 target gene expression, which was blocked by supplementation with the inhibitory Dll4-Fc peptide (Fig. 9 D). Again, LefΔN-βCTA significantly induced *Pdgfb* mRNA with and without Dll4 coating, and moreover, blockage of the Notch pathway by Dll4-Fc had no noticeable effect on *Pdgfb*, suggesting that its regulation by LefΔN-βCTA is Notch signaling independent.

GL261-derived Wnt1 up-regulates expression of PDGF-B in ECs in subcutaneous xenografts

To confirm the *Pdgfb* mRNA regulation by the Wnt/β-catenin pathway in tumor ECs in vivo, we performed ISH from Wnt1-GL261 tumors$^{+/-D}$, showing an increased

endothelial-specific signal for *Pdgfb* upon Wnt1 expression (Fig. 10 A). Furthermore, we mechanically isolated tumor vessels from Wnt1 tumors$^{+/-D}$ (Fig. 10 B). SDS-PAGE and Western blot revealed increased PDGF-B protein expression in vessels of Wnt1^{-D} tumors (Fig. 10 B).

DISCUSSION

The results of our present manuscript provide the first evidence for an antiangiogenic and vessel-normalizing role of endothelial Wnt/β-catenin signaling in glioma vascularization. As tumor vascularization is crucial for the progression of various types of malignancies (Saharinen et al., 2011), our findings will consolidate the understanding of pathological angiogenesis in general.

Comparing GL261 mouse glioma cells producing either Wnt1 or the soluble Wnt inhibitor Dkk1 in a DOX-inducible manner, we show that Wnt1 decreased and Dkk1 promoted tumor vascularization, leading to decreased and increased tumor growth, respectively. These findings were independently validated in a subcutaneous C6 rat glioma model constitutively expressing Wnt1 (not depicted). We also provide direct evidence that the tumor vasculature is targeted by glioma Wnt1, as indicated by increased nuclear β-catenin staining as the hallmark of β-catenin transcription. This finding is of particular importance as systemic treatments that activate the canonical Wnt pathway do not specifically target the endothelium. Moreover, we show that Wnt1-driven β-catenin signaling did not lead to increased GL261 and C6 tumor growth. Along this line, canonical Wnts, as opposed to the noncanonical Wnt5a, are not overexpressed in human GBM, suggesting that glioma cell–specific β-catenin signaling does not contribute to glioma initiation and progression. Interestingly, the canonical Wnt pathway has been described as antitumorigenic for glioma cells, making it, in combination with the vascular effects we report here, an interesting target to be activated for glioma therapy (Kotliarova et al., 2008).

The tumor phenotypes in Wnt1- and Dkk1-expressing tumors were comparable in the subcutaneous and intracranial transplantation models with some differences regarding vessel size. The latter might be explained

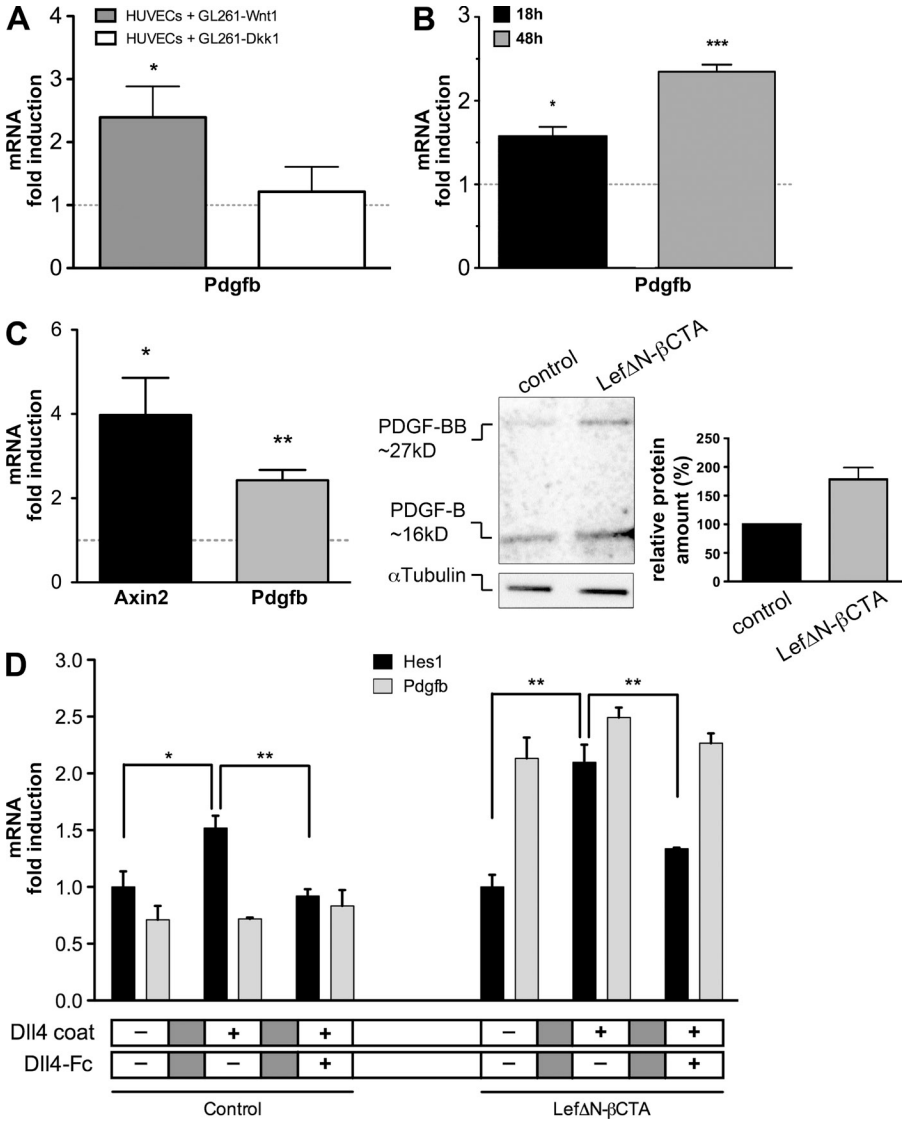

Figure 9. *Pdgfb* is a Notch-independent target of β-catenin signaling in ECs. (A) HUVECs co-cultivated with control^{-D}, Wnt1^{-D}, and Dkk1^{-D} GL261 cells. qRT-PCR ($n = 4$) for human *PDGFB* regulated by Wnt1^{-D} or Dkk1^{-D} (ns) compared with control^{-D} (gray line; *, $P < 0.05$). (B) qRT-PCR for *Pdgfb* gene regulated in MBEs stimulated by Wnt3aCM for 18 and 48 h compared with controlCM (gray line; $n = 4$; *, $P < 0.05$; ***, $P < 0.001$). (C, left) qRT-PCR for *Axin2* and *Pdgfb* regulated in β-catenin–deficient ECs transduced with LefΔN-βCTA compared with the vector control (gray line; $n = 4$; *, $P < 0.05$; **, $P < 0.01$). (right) Representative Western blot ($n = 1$) for PDGF-B from LefΔN-βCTA ECs compared with the vector control; top band shows the nonreduced (PDGF-BB) and bottom band reduced protein (PDGF-B). Densitometric analysis shows the summarized values for both forms of PDGF-B of samples loaded twice. (D) qRT-PCR of β-catenin–deficient ECs (control) or transduced with LefΔN-βCTA grown for 24 h either on gelatin- or Dll4-coated dishes ($n = 3$). Notch pathway induction was monitored by *Hes1* expression (*, $P < 0.05$; **, $P < 0.01$). Notch signaling was blocked by Dll4-Fc. Error bars indicate SEM.

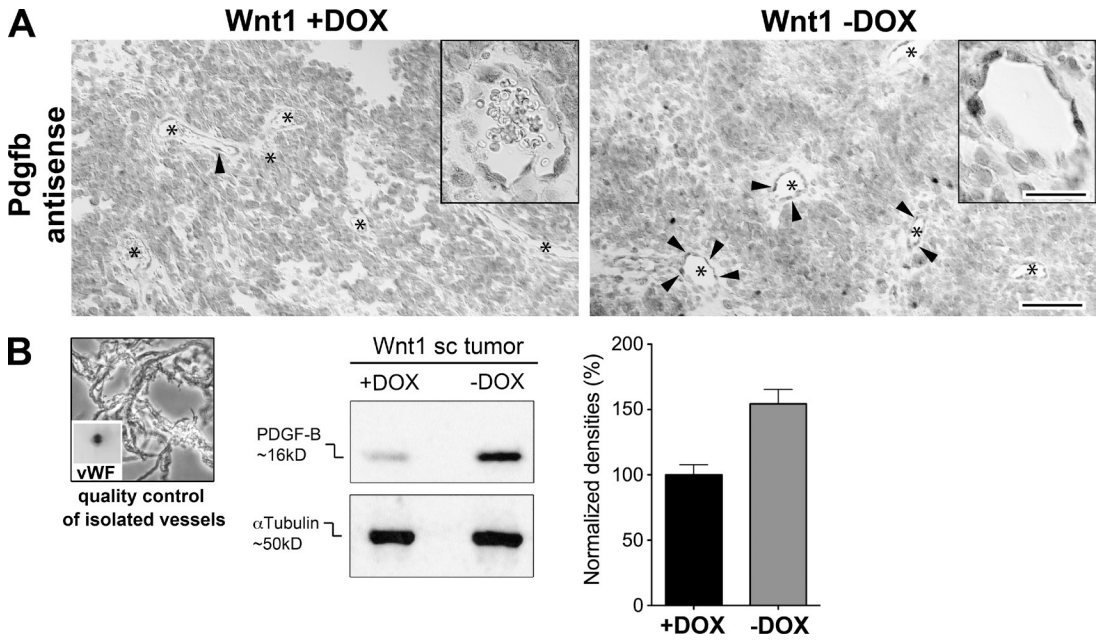

Figure 10. PDGF-B is up-regulated in the tumor endothelium upon Wnt1 expression. (A) Representative ISH for Pdgfb of subcutaneous Wnt1$^{+/-D}$ tumors. Asterisks indicate vessels, and arrowheads point to Pdgfb^{+} ECs. Insets show representative vessels in higher magnification. Bars: (full images) 50 µm; (insets) 18 µm. (B, left) Representative picture of isolated subcutaneous tumor vessels and dot blot for von Willebrand factor (vWF). (right) Representative Western blot for PDGF-B with pooled subcutaneous tumors vessels (n = 2 tumors/group). Densitometric analysis for PDGF-B of five independent Western blot experiments. Error bars indicate SEM.

by the diverging tumor microenvironment that has been shown by multiple studies comparing subcutaneous versus intracranial glioma growth (Arosarena et al., 1994; Blouw et al., 2003). As hypoxia and subsequent VEGF expression are major driving forces of tumor angiogenesis, we investigated the three different tumor conditions for hypoxic areas. Control^{-D} and Wnt1^{-D} subcutaneous tumors showed a similar hypoxic status, whereas Dkk1^{-D} tumors were almost devoid of hypoxia (Fig. 2 F). The finding that Dkk1^{-D} tumor vessels were functional regarding perfusion suggests that reduced hypoxia was a consequence of increased vascularity and oxygen supply (Fig. 3 E). As VEGF is a known target of Wnt signaling (Zhang et al., 2001), we tested the release of VEGF by the three GL261 glioma lines in vitro and observed higher levels of VEGF in Wnt1^{-D} compared with control^{-D} and Dkk1^{-D} glioma cells (not depicted).

Surprisingly, Wnt1^{-D} tumors showed reduced angiogenesis and normalized vessels given that these tumors were as hypoxic as the controls^{-D}, likely coinciding with high VEGF-A levels. These results suggest that reduced VEGF levels are not the cause of quiescent vessels in Wnt1^{-D} glioma. Furthermore, high VEGF expression in tumors is known to lead to SMC and PC drop off and to increase vessel permeability (Olsson et al., 2006). However, in Wnt1^{-D}-GL261 tumors, we observed decreased vascularization and an increased investment of α-SMA^{+}/desmin^{+} cells, speaking in favor of a diminished responsiveness of the endothelium to VEGF stimulation.

To mechanistically understand how endothelial Wnt/β-catenin signaling influences VEGF responsiveness, we focused on the cross talk of Wnt/β-catenin with Dll4/Notch as a vessel-stabilizing pathway. In this regard, Corada et al. (2010) recently provided evidence for the direct, transcriptional control of *Dll4* by β-catenin signaling during early embryonic angiogenesis, leading to a lack of vascular remodeling and of venous specification. Interestingly, the authors point out that no obvious effects of sustained Wnt/β-catenin signaling have been observed after midgestation, despite the fact that angiogenic processes were not complete.

In the present manuscript, we show for the first time that in pathological glioma angiogenesis, ECs become again responsive to the Wnt/β-catenin–Dll4 signaling axis. Specifically, endothelial-specific *Dll4* was up-regulated by glioma-derived Wnt1, leading to an inhibition of the angiogenic phenotype and thus to diminished tumor angiogenesis.

In control^{-D} and in particular in Dkk1^{-D} tumors, predominantly small, angiogenic vessels were *Dll4*+, supporting its role as a tip cell marker (Mailhos et al., 2001; Hellström et al., 2007). Interestingly, in Wnt1^{-D} tumor vessels, almost all ECs showed high Dll4 levels. It is known that Dll4 activates Notch signaling in adjacent ECs, influencing the levels of VEGFR expression (Hellström et al., 2007; Siekmann and Lawson, 2007), namely by lowering levels of VEGFR2 (Williams et al., 2006) and Nrp-1 (Gerhardt et al., 2004), thereby determining stalk cell identity. We show on a molecular level that the tip cell receptors *VEGFR2/flk1*, *VEGFR3/flt4*, and *Nrp1* were down-regulated and the stalk cell receptor *VEGFR1/flt1* was up-regulated upon Wnt/β-catenin signaling, suggesting the induction of a stalk cell–like gene signature. Along this

line, Jakobsson et al. (2010) showed that the tip cell identity is controlled by the relative availability of VEGFR2 and VEGFR1, which are downstream of Notch1.

The Notch ligand Jag1 is highly expressed in stalk cells, and its overexpression leads to Dll4/Notch1 inhibition and angiogenic sprouting in a fringe-dependent manner (Benedito et al., 2009). Interestingly, *Jag1* was also significantly up-regulated in ECs upon canonical Wnt signaling (Fig. 8, C and D). Although *Jag1* is a described Wnt target in the hair follicle (Estrach et al., 2006), our data support the interpretation that *Jag1* is not directly regulated by β-catenin, as *Jag1* together with *Notch1* were only induced after 48 h of Wnt3a stimulation, whereas direct Wnt targets such as *Axin2* and *Dll4* were already significantly regulated after 18 h (Fig. 8 D). It has also been reported that Dll4 coating leads to up-regulation of *JAG1* in HUVECs, strengthening the interpretation that *JAG1* is controlled by Notch signaling (Harrington et al., 2008).

Interestingly, we observed a slight but significant up-regulation of *JAG1* in the HUVEC co-culture model with $Dkk1^{-D}$ GL261 cells, whereas other Notch pathway genes remained unchanged. This finding underlines that the relative up-regulation of *Jag1* compared with *Dll4* might foster the angiogenic phenotype observed in $Dkk1^{-D}$ tumors (Benedito et al., 2009).

Segarra et al. (2008) have shown that artificial overexpression of Dll4 by BL41 lymphomas leads to reduced angiogenesis and tumor growth. Li et al. (2007) followed a similar approach by overexpressing Dll4 in five different tumor cell lines. They also observed a reduction in vessel density and increased vessel maturation; however, subcutaneous U87 human GBM grew significantly bigger compared with the controls. This suggests that there is a high degree of cell specificity for Dll4 concerning tumor cell response, whereas the endothelial response is apparently independent of the tumor type. Therefore, Dll4 might not be a good primary target in GBM but possibly in other malignancies.

Matrigel plug assays showed that the antiangiogenic effect of Wnt1 and the proangiogenic effect of Dkk1 are a consequence of endothelial-specific Wnt pathway activation and inhibition, respectively. Most relevant, the normalized vascular phenotype could be mimicked by endothelial-specific GOF for β-catenin in intracranial transplanted, parental GL261 glioma cells. Specifically, endothelial activation of β-catenin signaling (a) reduced tumor vessel density, (b) led to smooth deposition of ColIV to the vessel wall, and (c) resulted in thinner, more regular-shaped vessels and (d) increased vessel investment by PCs.

The latter have been shown to be important for vessel stability and barrier function in the brain (Armulik et al., 2010; Daneman et al., 2010). Consistently, we could show that permeability for endogenous mouse IgG was considerably lower in $Wnt1^{-D}$ compared with $Dkk1^{-D}$ or $control^{-D}$ glioma. In accordance with our previously described role of Wnt/β-catenin for BBB development (Liebner et al., 2008), we observed a partial rescue of junction protein localization in Wnt1-expressing tumors. This was even more remarkable, as Cldn3 has been shown to be one of the earliest junction proteins at the BBB that is down-regulated under pathological conditions (Liebner et al., 2000; Wolburg et al., 2003).

However, the central molecular finding of the present manuscript is that we provide the first evidence that the SMC/PC-attracting factor PDGF-B is regulated downstream of Wnt/β-catenin signaling in ECs. The regulation of *PDGFB* became apparent in HUVEC co-cultures with Wnt1-expressing GL261 cells and in Wnt3a stimulation of MBEs, speaking in favor of a direct regulation. Using the LefΔN-βCTA dominant-active signaling construct in β-catenin–deficient ECs, we establish *Pdgfb* to be directly regulated by the canonical Wnt pathway. Neither activation nor inhibition of Notch signaling in LefΔN-βCTA–transduced ECs affected Pdgfb up-regulation in vitro. ISH and Western blot analysis of tumor vessels corroborated the regulation of *Pdgfb* in Wnt1-expressing tumors contributing to SMC/PC recruitment.

The relevance of tumor vessel investment with SMCs/PCs for vessel normalization and tumor growth is strongly supported by the finding that PDGF-B–overexpressing colorectal tumors exhibit increased mural cell investment, normalized vessels, and reduced tumor growth (McCarty et al., 2007). Nevertheless, our results provide the first evidence for the direct regulation of PDGF-B by Wnt/β-catenin in ECs, as endothelial-derived PDGF-B is crucial for the proper recruitment of PCs (Abramsson et al., 2003).

However, PDGF-B has been proposed to be a tip cell marker but at the same time to be important for mural cell recruitment to stalk and phalanx cells (Gerhardt et al., 2003). Given that Wnt/β-catenin signaling has been suggested to be predominantly active in stalk cells (Phng et al., 2009), the regulation of PDGF-B downstream of β-catenin might contribute to the stalk cell behavior and vascular maturation. However, the exact mechanism of the cellular PDGF-B regulation in the context of tip and stalk cell identity needs further investigation.

Regarding mural cell investment and vessel stabilization, we did not observe regulation of human Angpt2 in HUVEC/GL261 co-cultures (Fig. 8 C). Instead, analysis of total RNA from subcutaneous glioma suggested a relative down-regulation of *Angpt2* in $Wnt1^{-D}$ tumors, supporting the observation of quiescent tumor vessels (not depicted). This might shift the balance toward *Angpt1*, in turn contributing to the stabilized vascular phenotype, as mural cell–derived Angpt1 seems to potentiate β-catenin signaling in ECs (Zhang et al., 2011).

Regarding the protumorigenic effect by Dkk1 overexpression from GL261 cells, it should be noted that Dkk1 has effects beyond mere inhibition of Wnt/β-catenin. Blocking Dll4 in a subcutaneous C6 rat glioma model has been shown to result in smaller sized tumors with increased vessel density caused by a nonfunctional tumor vascularization (Noguera-Troise et al., 2006). Interestingly, in the present work, tumor-derived Dkk1 resulted in hypervascularization by functional vessels, as revealed by isolectin perfusion, leading to reduced hypoxia (Figs. 2 F and 3 E) and thus increased

tumor growth. There is emerging evidence that Dkk1 drives mobilization and the angiogenic potential of endothelial precursor cells (Aicher et al., 2008; Smadja et al., 2010). Here we corroborate these data in a mouse glioma model, underlining a proangiogenic role of Dkk1. It should be noted that Min et al. (2011) proposed opposing function of Dkk1 and Dkk2, suggesting that Dkk1 confers anti- and Dkk2 proangiogenic properties. The apparent discrepancies between the data described by Min et al. (2011) and our data, which are in line with the data by Aicher et al. (2008) and Smadja et al. (2010), might be a result of the different experimental settings in vivo and in vitro. It should be noted that expression analysis of Dkk1 and Dkk2 in highly angiogenic human GBM supports a proangiogenic function of Dkk1, as it is up-regulated and Dkk2 is down-regulated compared with normal brain tissue (Fig. 1 A; Zhou et al., 2010). To conclusively describe the function of Dkk1 in angiogenesis, additional work needs to be done.

In summary, we demonstrate that continuously elevated Wnt/β-catenin signaling leads to the initial induction of *Dll4* and *Pdgfb*, followed by the acquisition of a stalk cell–specific gene signature downstream of elevated Notch signaling. Our findings might have multiple consequences for GBM therapy: (a) physiological levels of Wnt/β-catenin signaling are associated with angiogenesis and stalk cell proliferation, and (b) reinforced and sustained signaling leads to reduced angiogenesis independently of VEGF levels, with concomitant vessel normalization via Dll4 and PDGF-B expression, as well as junctional stabilization. As a consequence of the latter, endothelial Wnt/β-catenin partially rescues BBB disruption and prevents vasogenic edema. Collectively, these findings make the Wnt/β-catenin pathway an interesting target that could be exploited for antiangiogenic and/or antiedema therapy particularly in GBM but potentially also in other angiogenic tumors in the periphery such as melanoma (Lucero et al., 2010).

MATERIALS AND METHODS

Human GBM specimens. Biopsies of human glioma were provided by the University Cancer Center, Goethe University Frankfurt via M. Mittelbronn and P.N. Harter. We investigated five cases for each WHO grade I–IV of human glioma biopsies embedded in paraffin. Histological examination was performed by at least two experienced neuropathologists (M. Mittelbronn and P.N. Harter). Gene expression signatures were analyzed in 424 primary GBMs and 11 normal brain samples by assessing the TCGA data portal that used the 244K G4502A microarray (Agilent Technologies) to determine mRNA profiles for Wnt1, Wnt3a, Wnt5a, Wnt7a, Wnt7b, Dkk1, and Dkk2 to correlate the expression to normal brain (https://tcga-data.nci.nih.gov/tcga/tcgaHome2.jsp, accessed 2012 March 30; Cancer Genome Atlas Research Network, 2008). The raw data for the selected genes were downloaded and analyzed in Prism (GraphPad Software) to generate scatter blots. Utilization of all human specimens was in accordance with the ethics commissions of the Goethe University Clinic Frankfurt, Germany.

Cells. GL261 cells cultivated in D-MEM Media-GlutaMAX-I (Invitrogen) containing 10% FCS were stably transfected with pTet-Off plasmid using TransPass D1 Transfection Reagent (New England Biolabs, Inc.) and selected with 400 μg/ml G418. Tet-Off–responsive single cell clones were selected for stable transfection with the empty vector pTRE2hyg (control) or the vector containing either murine Wnt1 or human Dkk1 cDNA. Cells were selected with 200 μg/ml hygromycin B and cultivated in the presence of 1 μg/ml DOX. HUVECs were gifts from M. Tjwa (University Hospital Frankfurt, Frankfurt, Germany). MBEs were isolated, transformed with polyoma middle T, and cultivated as previously described (Liebner et al., 2008). β-Catenin–deficient endothelioma cells were generated and cultivated as previously described (Cattelino et al., 2003). Retroviral infection with LefΔN-βCTA subcloned in pBABE-puro was performed according to standard procedures (Liebner et al., 2004), and infected cells were selected by 4-μg/ml puromycin treatment for two splittings. As a vector control, the same parental β-catenin–deficient cell line was infected with the empty pBABE-puro vector, and cells were selected for puromycin resistance as described previously (Liebner et al., 2004).

Cell growth curve. 15×10^3 tumor cells were seeded in 24-well plates in the presence of DOX. After 24 h, medium was replaced by starving medium containing 1% BSA instead of 10% FCS. Again 24 h later, medium was changed with normal growth media selectively containing DOX. Living cells were identified by 0.04% Trypan blue solution (Sigma-Aldrich) and counted in a Neubauer chamber.

Reagents. Tamoxifen (free base) pellets (2 mg, 21-d release) were purchased from Innovative Research of America, Matrigel basement membrane matrix from BD, Heparin-Natrium 25000 from Ratiopharm, and bFGF from R&D Systems. Recombinant proteins were as follows: human Wnt1 (PeproTech), mouse Dkk1 as well as human Dll4 (R&D Systems), and Dll4 (mouse):Fc (human; rec.; AdipoGen). BCA Protein Assay kit was purchased from Thermo Fisher Scientific. Plasmids used were as follows: pTet-Off, pTRE2hyg, and pTRE2hyg-Luc (Takara Bio Inc.); pRL-TK (Promega); and pOTB7-human Dkk1 (IRAUp969H0447) and pYX-Asc-mouse Dll4 (IRAVp968E10130D; imaGenes). pcDNA3-mouse Wnt1 was a gift from G. Cossu (DIBIT San Raffaele Scientific Institute, Milan, Italy). Super(8×)TOP-FLASH and super(8×)FOP-FLASH were provided by R. Moon (University of Washington School of Medicine, Seattle, WA). ChromoMap red was purchased from VENTANA Medical Systems Inc. Monoclonal mouse antibodies used were as follows: anti–β-catenin clone14/β-catenin (BD), anti–α-SMA clone 1A4 Cy3-conjugated and anti–α-tubulin clone DM1A (Sigma-Aldrich), antipimonidazole FITC MaB 4.3.11.3 (NPI Inc.), anti-FITC MaB045P Ms X Fluor HRP (EMD Millipore), and rat anti–mouse CD31 (BD and Dianaova). Polyclonal antibodies used were as follows: rabbit anti–β-galactosidase (MP Biomedicals), rabbit anti-Clnd3 (Invitrogen), rabbit anti-ColIV (AbD Serotec), rabbit anti–PDGF-B (AB Biotec), and goat anti–human Dkk1, goat anti–mouse Podxl, and goat anti–mouse Wnt1 (R&D Systems). Secondary antibodies used were as follows: appropriated antibodies, streptavidin conjugates, and Alexa Fluor 488 and 568 conjugates (Invitrogen). For mouse IgG staining, a goat anti–mouse Alexa Fluor 488 antibody was used (Invitrogen). Mouse food containing 100 mg/kg DOX and control food was purchased from ssniff Spezialdiäten GmbH.

Luciferase reporter assay. To reveal canonical Wnt signaling, HEK293 cells were transfected with super(8×)TOP-FLASH or super(8×)FOP-FLASH. Firefly luciferase activity was normalized to Renilla luciferase by cotransfection with pRL-TK plasmid. All measurements were performed in a Lumat LB 9507 luminometer (Berthold Technologies).

qRT-PCR. Primers used for qRT-PCR are listed in Tables S1 and S2. RNA from cells was isolated with the RNeasy Mini kit from QIAGEN. qRT-PCR was performed as previously described (Schneider et al., 2010). For qRT-PCR analysis on HUVECs, G6pd1 and β-actin were used as human reference genes for normalization. qRT-PCR results are shown from at least three independent experiments (specified in figure legends).

Western blot analysis. For GL261 glioma cell analysis, 4×10^5 cells were cultured for 2 d in media supplemented either with or without DOX. Cells were harvested for Western blot analysis. Western blot was performed as previously described (Devraj et al., 2009; Schneider et al., 2010). In brief, ECs were harvested in 10 mM Hepes, 1 mM EDTA, and 250 mM sucrose plus protease inhibitor cocktail with final pH 7.4 (HES + PI), followed by mild sonication. Subsequently, BCA assay was performed and samples were stored

at −20°C. For Western blot, a buffer containing 2.3 M urea, 1.5% SDS, 15 mM Tris, 100 mM DTT, and 0.01% BPB (final concentrations) was added to the samples, and proteins were solubilized for 2 h at room temperature followed by SDS-PAGE.

The gels were then transferred by standard submerged method, followed by Western blotting for the indicated antibodies. The blots were visualized with the aid of an enhanced chemiluminescence kit, digitized into film images using an AlphaEase FC Imaging System (Alpha Innotech), and the densitometric images were then analyzed using Multi Gauge software 3.0 (Fujifilm). Quantitation was performed from 8-bit linear TIF images by selecting equal area from each sample lane that encompassed the band of interest and gray values obtained after subtracting the background from an empty lane. Densitometric measurement was performed on three separated blots for PDGF-B, normalized to α-tubulin, and shown as relative amounts in percentages.

Tumor experiments. All animal experiments were performed in accordance with the German Legislation on the Protections of Animals and the Guide for the Care and Use of Laboratory Animals with permission of the Regierungspräsidium Darmstadt (approval no. F94/10). Mice were anesthetized by i.p. injection of Ketamine/Xylazine, and 10^6 cells were implanted subcutaneously into the flanks of 6–8-wk-old female NUDE mice. Tumor volume was calculated by the formula $\pi/6 \times (\text{diam}^{\text{max}} \times \text{diam}^{\text{min}\wedge 2}$; Yoshio-Hoshino et al., 2007). Mice were sacrificed when a tumor diameter of 1.5 cm was reached. For DOX-dependent tumor experiments, mice were fed with DOX-containing food 2 wk before tumor cell transplantations. The DOX-containing diet was continued during tumor growth. Vessel isolation from subcutaneous tumors was performed as previously described for brain vessels, but omitting the dextran separation step (Fisher et al., 2007). For intracranial tumor transplantations, mice were inserted into a stereotactic device, and 10^5 cells (living cell number) in 2 µl PBS were injected into the striatum using the coordinates relative to bregma: 0.5 (anterior–posterior), 2 (mediolateral), and 3.5 (dorsoventral). Mice were sacrificed at once when showing symptoms. For β-catenin activation in vivo, Pdgfb-iCreERT2 (Claxton et al., 2008) lines were crossed to mice harboring floxed alleles of the β-catenin exon 3 to obtain homozygous β-catenin$^{\text{Exon3flox/flox}}$ mice (Harada et al., 1999), of which 50% also carried one Pdgfb-iCreERT2 allele. After intracranial transplantation of unmodified (parental) GL261 cells, a tamoxifen pellet was subcutaneously transplanted in the neck region of each mouse. Single transgenic Pdgfb-iCreERT2 heterozygous mice were treated in the same manner.

Tumor hypoxia detection and preparation of tumor material. To detect tumor hypoxia, 60 µg Hypoxyprobe per gram was injected i.p. 30 min before mice were sacrificed. Subcutaneous tumors were incubated overnight in 4% PFA, and one half was embedded in paraffin and the other half was infiltrated with 18% sucrose solution at 4°C overnight and embedded in O.C.T. Compound for cryosections. For intracranial tumors, brains were removed, incubated in 4% PFA at 4°C overnight, transferred into 0.1 M sodium phosphate buffer, pH 7.4, containing 30% sucrose, and incubated for several days at 4°C until complete infiltration and directly used to prepare thick sections (40 µm).

Tumor vessel perfusion experiments. 100 µg of biotinylated isolectin (Linaris) was administered retrobulbarily after mouse anesthesia 4 min before mice were perfused with 4% PFA. Subcutaneous tumors were divided in two halves, incubated overnight in 4% PFA, infiltrated with 18% sucrose solution at 4°C overnight, and embedded in O.C.T. Compound for cryosections.

Brain tumor volume calculation. Mouse brains containing intracranial tumors were harvested and used for sectioning after 30% sucrose buffer infiltration. For each brain, a row of 12 Eppendorf tubes was filled with cryoprotection solution (two parts 0.1 M sodium phosphate buffer, pH 7.4, mixed with one part ethylene glycol and one part glycerin). Serial thick sections (40 µm) starting from the olfactory bulb to the cerebellum were performed. Every brain slice was consecutively placed in one Eppendorf tube starting with tube 1 and ending with tube 12. This procedure was repeated until the whole brain was cut. For brain tumor volume calculation, the brain slices of one tube were transferred on slides for H&E staining. Tumor area of every slice was evaluated with an Axiophot microscope (Carl Zeiss) with a motorized stage, equipped with a Hitachi HV-C20A camera and the Stereo Investigator 4.3.4 software (MicrcoBrightField, Inc.). The following formula was used to calculate brain tumor volume: tumor volume = slice size (40 µm) × step size between the slices (12) × sum of tumor areas from one tube.

Matrigel plug assay. 1 ml Matrigel basement membrane matrix was mixed with 30 U Heparin-Natrium 25000, and 1 µg bFGF and supplemented either with 400 µg human Wnt1 or 200 µg mouse Dkk1 recombinant protein or with an equivalent volume of PBS with 0.1% BSA (control). 500 µl Matrigel mixture was injected subcutaneously into 6–8-wk-old C57BL/6 mice. After 7 d, plugs were excised, fixed overnight in 10% formaldehyde, and embedded in paraffin.

Immunohistochemical and immunofluorescence (IF) analysis. H&E staining was performed on paraffin sections or 40-µm brain thick sections. Matrigel paraffin sections were stained for CD31/PECAM-1 in aVENTANA Discovery XT staining device. IF staining was either performed on 4% PFA fixed cryosections (12 µm) or brain thick sections (40 µm). For staining of Cldn3, Cldn5, and ZO-1, 10-µm brain cryosections were fixed with 95% ethanol for 5 min at 4°C followed by acetone incubation for 1 min at room temperature. Light and IF microscopic images were observed either with an 80i microscope and documented with a digital DS-5Mc camera or with a C1si confocal microscope (Nikon). Images were computer processed in ImageJ (National Institutes of Health) and Photoshop CS4 for Macintosh (Adobe). Vessel density, vessel size, and hypoxic areas were determined with NIS Elements AR Imaging Software (Nikon). ISH against mouse Dll4 and mouse Pdgfb (provided by H. Gerhardt, Cancer Research UK, London, England, UK) was performed on subcutaneous paraffin tumor slices as previously described (Schneider et al., 2010).

GL261/HUVEC co-culture experiment. 8×10^5 control-, Wnt1-, and Dkk1-GL261 cells were cultivated for 2 d on 0.1% gelatin–coated 60-mm dishes. 6×10^5 HUVECs were seeded on the tumor cells, and RNA was harvested after 24 h.

Stimulation of MBEs. 3×10^5 MBEs were seeded on 0.1% gelatin-coated 6-well plates. Control or Wnt3aCM derived from L cells was diluted 1:1 with EC growth medium (Liebner et al., 2008). RNA was harvested after 18 h and 48 h of stimulation, respectively.

Dll4 stimulation and inhibition of Notch signaling. 4×10^5 β-catenin–deficient ECs transduced with either pBABE-puro/LefΔN-βCTA or the control vector were seeded on 0.1% gelatin-coated 6-well plates containing 500 ng/ml human recombinant Dll4 for the stimulation condition. To inhibit Notch signaling, 5 µg/ml Dll4 (mouse):FC (human; rec.) was added when seeding the cells (Lobov et al., 2011). RNA was harvested after 24 h of cultivation.

Statistical analysis. Results are shown as the mean ± SEM. A two-tailed, unpaired Student's *t* test for pairwise comparison was used (Prism version 5.0a; GraphPad Software). P-values <0.05 were considered significant (***, <0.001; **, 0.001–0.01; *, 0.01–0.05).

Online supplemental material. Videos 1 and 2 show the distribution of ColIV around the Podxl$^+$ vessel in intracranial control and β-catenin GOF tumors, respectively. Videos 3 and 4 show the attachment of desmin$^+$ PCs around the CD31$^+$ vessel in intracranial control and β-catenin GOF tumors, respectively. Tables S1 and S2 provide mouse and human qRT-PCR primer sequences, respectively. Online supplemental material is available at http://www.jem.org/cgi/content/full/jem.20111580/DC1.

We thank Janina Drynski and Tino Röxe for excellent technical support. We are grateful to Stefanie Gelhardt for excellent animal husbandry, Prof. Dr. Michel Mittelbronn and Dr. Patrick Harter for discussions and support in TCGA analysis, and Dr. Holger Gerhardt for providing the Pdgfb in situ probes.

This study has been supported by the Deutsche Forschungsgemeinschaft (SFB/TR23 B7 "Vascular Differentiation and Remodeling" to S. Liebner and K.H. Plate and the

Forschergruppe 527 "Suszeptibilitätsfaktoren der Tumorgenese" to E. Bockamp), the LOEWE Initiative Hessen (Onkogene Signaltransduktion Frankfurt, III L 4-518/55.004, 2009 to S. Liebner and K.H. Plate), the Excellence Cluster Cardio-Pulmonary System (to S. Liebner and K.H. Plate), and European Union Health FP7 (JUSTBRAIN to S. Liebner and K.H. Plate).

The authors have no conflicting financial interests.

Submitted: 29 July 2011
Accepted: 23 July 2012

REFERENCES

Abramsson, A., P. Lindblom, and C. Betsholtz. 2003. Endothelial and nonendothelial sources of PDGF-B regulate pericyte recruitment and influence vascular pattern formation in tumors. *J. Clin. Invest.* 112:1142–1151.

Adams, R.H., and K. Alitalo. 2007. Molecular regulation of angiogenesis and lymphangiogenesis. *Nat. Rev. Mol. Cell Biol.* 8:464–478. http://dx.doi.org/10.1038/nrm2183

Aicher, A., O. Kollet, C. Heeschen, S. Liebner, C. Urbich, C. Ihling, A. Orlandi, T. Lapidot, A.M. Zeiher, and S. Dimmeler. 2008. The Wnt antagonist Dickkopf-1 mobilizes vasculogenic progenitor cells via activation of the bone marrow endosteal stem cell niche. *Circ. Res.* 103:796–803. http://dx.doi.org/10.1161/CIRCRESAHA.107.172718

Armulik, A., G. Genové, M. Mäe, M.H. Nisancioglu, E. Wallgard, C. Niaudet, L. He, J. Norlin, P. Lindblom, K. Strittmatter, et al. 2010. Pericytes regulate the blood-brain barrier. *Nature.* 468:557–561. http://dx.doi.org/10.1038/nature09522

Arosarena, O., C. Guerin, H. Brem, and J. Laterra. 1994. Endothelial differentiation in intracerebral and subcutaneous experimental gliomas. *Brain Res.* 640:98–104. http://dx.doi.org/10.1016/0006-8993(94)91861-9

Augustin, I., V. Goidts, A. Bongers, G. Kerr, G. Vollert, B. Radlwimmer, C. Hartmann, C. Herold-Mende, G. Reifenberger, A. von Deimling, and M. Boutros. 2012. The Wnt secretion protein Evi/Gpr177 promotes glioma tumourigenesis. *EMBO Mol. Med.* 4:38–51. http://dx.doi.org/10.1002/emmm.201100186

Benedito, R., C. Roca, I. Sörensen, S. Adams, A. Gossler, M. Fruttiger, and R.H. Adams. 2009. The notch ligands Dll4 and Jagged1 have opposing effects on angiogenesis. *Cell.* 137:1124–1135. http://dx.doi.org/10.1016/j.cell.2009.03.025

Bergers, G., and L.E. Benjamin. 2003. Tumorigenesis and the angiogenic switch. *Nat. Rev. Cancer.* 3:401–410. http://dx.doi.org/10.1038/nrc1093

Blouw, B., H. Song, T. Tihan, J. Bosze, N. Ferrara, H.P. Gerber, R.S. Johnson, and G. Bergers. 2003. The hypoxic response of tumors is dependent on their microenvironment. *Cancer Cell.* 4:133–146. http://dx.doi.org/10.1016/S1535-6108(03)00194-6

Brastianos, P.K., and T.T. Batchelor. 2009. VEGF inhibitors in brain tumors. *Clin. Adv. Hematol. Oncol.* 7:753–760: 768.

Cancer Genome Atlas Research Network. 2008. Comprehensive genomic characterization defines human glioblastoma genes and core pathways. *Nature.* 455:1061–1068. http://dx.doi.org/10.1038/nature07385

Carmeliet, P., and R.K. Jain. 2011. Principles and mechanisms of vessel normalization for cancer and other angiogenic diseases. *Nat. Rev. Drug Discov.* 10:417–427. http://dx.doi.org/10.1038/nrd3455

Cattelino, A., S. Liebner, R. Gallini, A. Zanetti, G. Balconi, A. Corsi, P. Bianco, H. Wolburg, R. Moore, B. Oreda, et al. 2003. The conditional inactivation of the β-catenin gene in endothelial cells causes a defective vascular pattern and increased vascular fragility. *J. Cell Biol.* 162:1111–1122. http://dx.doi.org/10.1083/jcb.200212157

Chien, A.J., W.H. Conrad, and R.T. Moon. 2009. A Wnt survival guide: from flies to human disease. *J. Invest. Dermatol.* 129:1614–1627. http://dx.doi.org/10.1038/jid.2008.445

Claxton, S., V. Kostourou, S. Jadeja, P. Chambon, K. Hodivala-Dilke, and M. Fruttiger. 2008. Efficient, inducible Cre-recombinase activation in vascular endothelium. *Genesis.* 46:74–80. http://dx.doi.org/10.1002/dvg.20367

Corada, M., D. Nyqvist, F. Orsenigo, A. Caprini, C. Giampietro, M.M. Taketo, M.L. Iruela-Arispe, R.H. Adams, and E. Dejana. 2010. The Wnt/beta-catenin pathway modulates vascular remodeling and specification by upregulating Dll4/Notch signaling. *Dev. Cell.* 18:938–949. http://dx.doi.org/10.1016/j.devcel.2010.05.006

Daneman, R., D. Agalliu, L. Zhou, F. Kuhnert, C.J. Kuo, and B.A. Barres. 2009. Wnt/beta-catenin signaling is required for CNS, but not non-CNS, angiogenesis. *Proc. Natl. Acad. Sci. USA.* 106:641–646. http://dx.doi.org/10.1073/pnas.0805165106

Daneman, R., L. Zhou, A.A. Kebede, and B.A. Barres. 2010. Pericytes are required for blood-brain barrier integrity during embryogenesis. *Nature.* 468:562–566. http://dx.doi.org/10.1038/nature09513

Devraj, K., R. Geguchadze, M.E. Klinger, W.M. Freeman, A. Mokashi, R.A. Hawkins, and I.A. Simpson. 2009. Improved membrane protein solubilization and clean-up for optimum two-dimensional electrophoresis utilizing GLUT-1 as a classic integral membrane protein. *J. Neurosci. Methods.* 184:119–123. http://dx.doi.org/10.1016/j.jneumeth.2009.07.016

Estrach, S., C.A. Ambler, C. Lo Celso, K. Hozumi, and F.M. Watt. 2006. Jagged 1 is a beta-catenin target gene required for ectopic hair follicle formation in adult epidermis. *Development.* 133:4427–4438. http://dx.doi.org/10.1242/dev.02644

Fisher, J., K. Devraj, J. Ingram, B. Slagle-Webb, A.B. Madhankumar, X. Liu, M. Klinger, I.A. Simpson, and J.R. Connor. 2007. Ferritin: a novel mechanism for delivery of iron to the brain and other organs. *Am. J. Physiol. Cell Physiol.* 293:C641–C649. http://dx.doi.org/10.1152/ajpcell.00599.2006

Franco, C.A., S. Liebner, and H. Gerhardt. 2009. Vascular morphogenesis: a Wnt for every vessel? *Curr. Opin. Genet. Dev.* 19:476–483. http://dx.doi.org/10.1016/j.gde.2009.09.004

Gerhardt, H., M. Golding, M. Fruttiger, C. Ruhrberg, A. Lundkvist, A. Abramsson, M. Jeltsch, C. Mitchell, K. Alitalo, D. Shima, and C. Betsholtz. 2003. VEGF guides angiogenic sprouting utilizing endothelial tip cell filopodia. *J. Cell Biol.* 161:1163–1177. http://dx.doi.org/10.1083/jcb.200302047

Gerhardt, H., C. Ruhrberg, A. Abramsson, H. Fujisawa, D. Shima, and C. Betsholtz. 2004. Neuropilin-1 is required for endothelial tip cell guidance in the developing central nervous system. *Dev. Dyn.* 231:503–509. http://dx.doi.org/10.1002/dvdy.20148

Harada, N., Y. Tamai, T. Ishikawa, B. Sauer, K. Takaku, M. Oshima, and M.M. Taketo. 1999. Intestinal polyposis in mice with a dominant stable mutation of the beta-catenin gene. *EMBO J.* 18:5931–5942. http://dx.doi.org/10.1093/emboj/18.21.5931

Harrington, L.S., R.C.A. Sainson, C.K. Williams, J.M. Taylor, W. Shi, J.-L. Li, and A.L. Harris. 2008. Regulation of multiple angiogenic pathways by Dll4 and Notch in human umbilical vein endothelial cells. *Microvasc. Res.* 75:144–154. http://dx.doi.org/10.1016/j.mvr.2007.06.006

Hellström, M., L.K. Phng, J.J. Hofmann, E. Wallgard, L. Coultas, P. Lindblom, J. Alva, A.K. Nilsson, L. Karlsson, N. Gaiano, et al. 2007. Dll4 signalling through Notch1 regulates formation of tip cells during angiogenesis. *Nature.* 445:776–780. http://dx.doi.org/10.1038/nature05571

Jakobsson, L., C.A. Franco, K. Bentley, R.T. Collins, B. Ponsioen, I.M. Aspalter, I. Rosewell, M. Busse, G. Thurston, A. Medvinsky, et al. 2010. Endothelial cells dynamically compete for the tip cell position during angiogenic sprouting. *Nat. Cell Biol.* 12:943–953. http://dx.doi.org/10.1038/ncb2103

Kamino, M., M. Kishida, T. Kibe, K. Ikoma, M. Iijima, H. Hirano, M. Tokudome, L. Chen, C. Koriyama, K. Yamada, et al. 2011. Wnt-5a signaling is correlated with infiltrative activity in human glioma by inducing cellular migration and MMP-2. *Cancer Sci.* 102:540–548. http://dx.doi.org/10.1111/j.1349-7006.2010.01815.x

Kotliarova, S., S. Pastorino, L.C. Kovell, Y. Kotliarov, H. Song, W. Zhang, R. Bailey, D. Maric, J.C. Zenklusen, J. Lee, and H.A. Fine. 2008. Glycogen synthase kinase-3 inhibition induces glioma cell death through c-MYC, nuclear factor-kappaB, and glucose regulation. *Cancer Res.* 68:6643–6651. http://dx.doi.org/10.1158/0008-5472.CAN-08-0850

Li, J.L., R.C. Sainson, W. Shi, R. Leek, L.S. Harrington, M. Preusser, S. Biswas, H. Turley, E. Heikamp, J.A. Hainfellner, and A.L. Harris. 2007. Delta-like 4 Notch ligand regulates tumor angiogenesis, improves tumor vascular function, and promotes tumor growth in vivo. *Cancer Res.* 67:11244–11253. http://dx.doi.org/10.1158/0008-5472.CAN-07-0969

Liebner, S., and K.H. Plate. 2010. Differentiation of the brain vasculature: the answer came blowing by the Wnt. *J. Angiogenes Res.* 2:1. http://dx.doi.org/10.1186/2040-2384-2-1

Liebner, S., A. Fischmann, G. Rascher, F. Duffner, E.H. Grote, H. Kalbacher, and H. Wolburg. 2000. Claudin-1 and claudin-5 expression

and tight junction morphology are altered in blood vessels of human glioblastoma multiforme. *Acta Neuropathol.* 100:323–331. http://dx.doi.org/10.1007/s004010000180

Liebner, S., A. Cattelino, R. Gallini, N. Rudini, M. Iurlaro, S. Piccolo, and E. Dejana. 2004. β-Catenin is required for endothelial-mesenchymal transformation during heart cushion development in the mouse. *J. Cell Biol.* 166:359–367. http://dx.doi.org/10.1083/jcb.200403050

Liebner, S., M. Corada, T. Bangsow, J. Babbage, A. Taddei, C.J. Czupalla, M. Reis, A. Felici, H. Wolburg, M. Fruttiger, et al. 2008. Wnt/β-catenin signaling controls development of the blood–brain barrier. *J. Cell Biol.* 183:409–417. http://dx.doi.org/10.1083/jcb.200806024

Lobov, I.B., R.A. Renard, N. Papadopoulos, N.W. Gale, G. Thurston, G.D. Yancopoulos, and S.J. Wiegand. 2007. Delta-like ligand 4 (Dll4) is induced by VEGF as a negative regulator of angiogenic sprouting. *Proc. Natl. Acad. Sci. USA.* 104:3219–3224. http://dx.doi.org/10.1073/pnas.0611206104

Lobov, I.B., E. Cheung, R. Wudali, J. Cao, G. Halasz, Y. Wei, A. Economides, H.C. Lin, N. Papadopoulos, G.D. Yancopoulos, and S.J. Wiegand. 2011. The Dll4/Notch pathway controls postangiogenic blood vessel remodeling and regression by modulating vasoconstriction and blood flow. *Blood.* 117:6728–6737. http://dx.doi.org/10.1182/blood-2010-08-302067

Lucero, O.M., D.W. Dawson, R.T. Moon, and A.J. Chien. 2010. A re-evaluation of the "oncogenic" nature of Wnt/beta-catenin signaling in melanoma and other cancers. *Curr. Oncol. Rep.* 12:314–318. http://dx.doi.org/10.1007/s11912-010-0114-3

Machein, M., and L.S. de Miguel. 2009. Angiogenesis in gliomas. *Recent Results Cancer Res.* 171:193–215. http://dx.doi.org/10.1007/978-3-540-31206-2_12

Mailhos, C., U. Modlich, J. Lewis, A. Harris, R. Bicknell, and D. Ish-Horowicz. 2001. Delta4, an endothelial specific notch ligand expressed at sites of physiological and tumor angiogenesis. *Differentiation.* 69:135–144. http://dx.doi.org/10.1046/j.1432-0436.2001.690207.x

McCarty, M.F., R.J. Somcio, O. Stoeltzing, J. Wey, F. Fan, W. Liu, C. Bucana, and L.M. Ellis. 2007. Overexpression of PDGF-BB decreases colorectal and pancreatic cancer growth by increasing tumor pericyte content. *J. Clin. Invest.* 117:2114–2122. http://dx.doi.org/10.1172/JCI31334

Min, J.-K., H. Park, H.-J. Choi, Y. Kim, B.-J. Pyun, V. Agrawal, B.-W. Song, J. Jeon, Y.-S. Maeng, S.-S. Rho, et al. 2011. The WNT antagonist Dickkopf2 promotes angiogenesis in rodent and human endothelial cells. *J. Clin. Invest.* 121:1882–1893. http://dx.doi.org/10.1172/JCI42556

Noguera-Troise, I., C. Daly, N.J. Papadopoulos, S. Coetzee, P. Boland, N.W. Gale, H.C. Lin, G.D. Yancopoulos, and G. Thurston. 2006. Blockade of Dll4 inhibits tumour growth by promoting non-productive angiogenesis. *Nature.* 444:1032–1037. http://dx.doi.org/10.1038/nature05355

Olsson, A.-K., A. Dimberg, J. Kreuger, and L. Claesson-Welsh. 2006. VEGF receptor signalling - in control of vascular function. *Nat. Rev. Mol. Cell Biol.* 7:359–371. http://dx.doi.org/10.1038/nrm1911

Phng, L.K., and H. Gerhardt. 2009. Angiogenesis: a team effort coordinated by notch. *Dev. Cell.* 16:196–208. http://dx.doi.org/10.1016/j.devcel.2009.01.015

Phng, L.K., M. Potente, J.D. Leslie, J. Babbage, D. Nyqvist, I. Lobov, J.K. Ondr, S. Rao, R.A. Lang, G. Thurston, and H. Gerhardt. 2009. Nrarp coordinates endothelial Notch and Wnt signaling to control vessel density in angiogenesis. *Dev. Cell.* 16:70–82. http://dx.doi.org/10.1016/j.devcel.2008.12.009

Saharinen, P., L. Eklund, K. Pulkki, P. Bono, and K. Alitalo. 2011. VEGF and angiopoietin signaling in tumor angiogenesis and metastasis. *Trends Mol. Med.* 17:347–362. http://dx.doi.org/10.1016/j.molmed.2011.01.015

Schneider, F.T., A. Schänzer, C.J. Czupalla, S. Thom, K. Engels, M.H. Schmidt, K.H. Plate, and S. Liebner. 2010. Sonic hedgehog acts as a negative regulator of beta-catenin signaling in the adult tongue epithelium. *Am. J. Pathol.* 177:404–414. http://dx.doi.org/10.2353/ajpath.2010.091079

Segarra, M., C.K. Williams, Mde.L. Sierra, M. Bernardo, P.J. McCormick, D. Maric, C. Regino, P. Choyke, and G. Tosato. 2008. Dll4 activation of Notch signaling reduces tumor vascularity and inhibits tumor growth. *Blood.* 112:1904–1911. http://dx.doi.org/10.1182/blood-2007-11-126045

Siekmann, A.F., and N.D. Lawson. 2007. Notch signalling limits angiogenic cell behaviour in developing zebrafish arteries. *Nature.* 445:781–784. http://dx.doi.org/10.1038/nature05577

Smadja, D.M., C. d'Audigier, L.-B. Weiswald, C. Badoual, V. Dangles-Marie, L. Mauge, S. Evrard, I. Laurendeau, F. Lallemand, S. Germain, et al. 2010. The Wnt antagonist Dickkopf-1 increases endothelial progenitor cell angiogenic potential. *Arterioscler. Thromb. Vasc. Biol.* 30:2544–2552. http://dx.doi.org/10.1161/ATVBAHA.110.213751

Smolich, B.D., J.A. McMahon, A.P. McMahon, and J. Papkoff. 1993. Wnt family proteins are secreted and associated with the cell surface. *Mol. Biol. Cell.* 4:1267–1275.

Stenman, J.M., J. Rajagopal, T.J. Carroll, M. Ishibashi, J. McMahon, and A.P. McMahon. 2008. Canonical Wnt signaling regulates organ-specific assembly and differentiation of CNS vasculature. *Science.* 322:1247–1250. http://dx.doi.org/10.1126/science.1164594

Streit, M., and M. Detmar. 2003. Angiogenesis, lymphangiogenesis, and melanoma metastasis. *Oncogene.* 22:3172–3179. http://dx.doi.org/10.1038/sj.onc.1206457

Thomas, M., and H.G. Augustin. 2009. The role of the Angiopoietins in vascular morphogenesis. *Angiogenesis.* 12:125–137. http://dx.doi.org/10.1007/s10456-009-9147-3

Vleminckx, K., R. Kemler, and A. Hecht. 1999. The C-terminal transactivation domain of beta-catenin is necessary and sufficient for signaling by the LEF-1/beta-catenin complex in *Xenopus laevis*. *Mech. Dev.* 81:65–74. http://dx.doi.org/10.1016/S0925-4773(98)00225-1

Willert, K., J.D. Brown, E. Danenberg, A.W. Duncan, I.L. Weissman, T. Reya, J.R. Yates III, and R. Nusse. 2003. Wnt proteins are lipid-modified and can act as stem cell growth factors. *Nature.* 423:448–452. http://dx.doi.org/10.1038/nature01611

Williams, C.K., J.-L. Li, M. Murga, A.L. Harris, and G. Tosato. 2006. Up-regulation of the Notch ligand Delta-like 4 inhibits VEGF-induced endothelial cell function. *Blood.* 107:931–939. http://dx.doi.org/10.1182/blood-2005-03-1000

Wolburg, H., K. Wolburg-Buchholz, J. Kraus, G. Rascher-Eggstein, S. Liebner, S. Hamm, F. Duffner, E.H. Grote, W. Risau, and B. Engelhardt. 2003. Localization of claudin-3 in tight junctions of the blood-brain barrier is selectively lost during experimental autoimmune encephalomyelitis and human glioblastoma multiforme. *Acta Neuropathol.* 105:586–592.

Yano, H., A. Hara, J. Shinoda, K. Takenaka, N. Yoshimi, H. Mori, and N. Sakai. 2000a. Immunohistochemical analysis of beta-catenin in N-ethyl-N-nitrosourea-induced rat gliomas: implications in regulation of angiogenesis. *Neurol. Res.* 22:527–532.

Yano, H., A. Hara, K. Takenaka, K. Nakatani, J. Shinoda, K. Shimokawa, N. Yoshimi, H. Mori, and N. Sakai. 2000b. Differential expression of beta-catenin in human glioblastoma multiforme and normal brain tissue. *Neurol. Res.* 22:650–656.

Yoshio-Hoshino, N., Y. Adachi, C. Aoki, A. Pereboev, D.T. Curiel, and N. Nishimoto. 2007. Establishment of a new interleukin-6 (IL-6) receptor inhibitor applicable to the gene therapy for IL-6-dependent tumor. *Cancer Res.* 67:871–875. http://dx.doi.org/10.1158/0008-5472.CAN-06-3641

Zhang, J., S. Fukuhara, K. Sako, T. Takenouchi, H. Kitani, T. Kume, G.Y. Koh, and N. Mochizuki. 2011. Angiopoietin-1/Tie2 signal augments basal Notch signal controlling vascular quiescence by inducing delta-like 4 expression through AKT-mediated activation of beta-catenin. *J. Biol. Chem.* 286:8055–8066. http://dx.doi.org/10.1074/jbc.M110.192641

Zhang, X., J.P. Gaspard, and D.C. Chung. 2001. Regulation of vascular endothelial growth factor by the Wnt and K-ras pathways in colonic neoplasia. *Cancer Res.* 61:6050–6054.

Zhou, Y., F. Liu, Q. Xu, and X. Wang. 2010. Analysis of the expression profile of Dickkopf-1 gene in human glioma and the association with tumor malignancy. *J. Exp. Clin. Cancer Res.* 29:138. http://dx.doi.org/10.1186/1756-9966-29-138